U.S.NRC
United States Nuclear Regulatory Commission
Protecting People and the Environment

Technical Letter Report
TLR-RES/DE/MEB-2025-05
PNNL-37470

Alloy 182 and Alloy 600 PWSCC Initiation Testing Status 2024

September 2025

Prepared by:

Mychailo B. Toloczko, Ziqing Zhai, and Jing Wang

Pacific Northwest National Laboratory

NRC Project Manager:

Eric M. Focht
Materials Engineering Branch

Division of Engineering
Office of Nuclear Regulatory Research
U.S. Nuclear Regulatory Commission
Rockville, MD 20852

This report does not contain or imply legally binding requirements. Nor does this report establish or modify any regulatory guidance or positions of the U.S. Nuclear Regulatory Commission and is not binding on the Commission.

Pacific Northwest
NATIONAL LABORATORY

PNNL-37470

Alloy 182 and Alloy 600 PWSCC Initiation Testing Status 2024

September 2025

Mychailo B. Toloczko
Ziqing Zhai
Jing Wang

Prepared for the U.S. Nuclear Regulatory Commission
Office of Nuclear Regulatory Research
Under Contract DE-AC05-76RL01830
Interagency Agreement: GT&C A2307-031-089-048662
NRC Agreement 31310024S0015

DISCLAIMER

PACIFIC NORTHWEST NATIONAL LABORATORY
operated by
BATTELLE
for the
UNITED STATES DEPARTMENT OF ENERGY
under Contract DE-AC05-76RL01830

PNNL-37470

Alloy 182 and Alloy 600 PWSCC Initiation Testing Status 2024

September 2025

Mychailo B. Toloczko
Ziqing Zhai
Jing Wang

Prepared for the U.S. Nuclear Regulatory Commission
Office of Nuclear Regulatory Research
Under Contract DE-AC05-76RL01830
Interagency Agreement: GT&C A2307-031-089-048662

Pacific Northwest National Laboratory
Richland, Washington 99354

Abstract

This document provides a summary of Alloy 182 and Alloy 600 testing results obtained from 2020 through the end of 2024. For Alloy 182, new tests were completed to provide information about the dependence of Alloy 182 stress corrosion crack initiation on temperature, dissolved hydrogen (DH), and mode of cold deformation. Although tests are still ongoing, many observations are possible.

With regard to Alloy 182 temperature effects, it was found that the substantial tail to long initiation times that was consistently observed during testing at 360°C vanishes as test temperature is reduced. At 300°C, the tail of the distribution of initiation times had completely vanished. The change in the shape of the distribution of SCCI values as a function of temperature results in a negative activation energy when using average SCCI time at each test temperature. Using the median and mode values results in a positive activation energy.

Results obtained thus far on Alloy 182 DH effects generally mirror results obtained by other researchers on Alloy 600. In the NiO-stable regime, crack initiation times are trending to higher values, while in the Ni-metal stable regime, crack initiation times are consistently low.

The effect of deformation on Alloy 182 stress corrosion crack initiation is being assessed by comparing crack initiation times for cold forged (in compression) and cold tensile strained material. The work completed thus far reveals that crack initiation times drop much more dramatically as a function of cold work level for the cold forged material. As a result, Alloy 182 crack initiation stress dependence is much different between the two modes of deformation. Cold forged material has a much larger stress exponent than cold tensile strained material.

Alloy 600 testing has focused on evaluating the effect of sub-yield stress loads on stress corrosion crack initiation. Two heats of material in a 15% cold forged condition readily exhibited crack initiation down to the lowest evaluated stress level, which was 80% of the yield stress. Not only does this provide information about Alloy 600 behavior, but it also provides context for the sub-yield stress crack initiations on Alloy 182 provided in the 2021 report where it was observed that 15% CF Alloy 182 tested at 90% of its yield stress exhibited approximately 100 times longer initiation times than the same material tested at 100% of its yield stress.

Acronyms and Abbreviations

BOC	beginning of cycle
CF	cold forged
CTS	cold tensile strained
DCPD	direct current potential drop
DDC	ductility dip crack
DH	dissolved hydrogen
DOE	U.S. Department of Energy
DOE-NE	U.S. Department of Energy Office of Nuclear Energy
EdF	Électricité de France
EMI	electromagnetic interference
EPRI	Electric Power Research Institute
EWI	Edison Welding Institute
IGA	intergranular attack
KAPL	Knolls Atomic Power Laboratory
LWR	light water reactor
LWRS	Light Water Reactor Sustainability (Program)
NRC	U.S. Nuclear Regulatory Commission
PNNL	Pacific Northwest National Laboratory
PWR	pressurized water reactor
PWSCC	primary water stress corrosion cracking
SCC	stress corrosion crack(ing)
SCCGR	stress corrosion crack growth rate
SCCI	stress corrosion crack initiation
SEM	scanning electron microscopy
SNR	signal-to-noise ratio
xLPR	Extremely Low Probability of Rupture Program
YS	yield stress

Contents

List of Figures

List of Tables

1.0 Introduction

This report covers progress on ongoing stress corrosion crack initiation (SCCI) testing of Alloys 182 and 600. Alloy 182 SCCI data supports factor of improvement (FOI) determination for Alloys 152(M)/52(M) and is generating environmental and material dependencies for Alloy 182 SCCI times for validation and future refinements of the models that were developed under the Extremely Low Probability of Rupture (xLPR) Program, which is a collaborative effort between the U.S. Nuclear Regulatory Commission (NRC) and Electric Power Research Institute (EPRI). To accomplish these goals, the NRC and EPRI have, through a Memorandum of Understanding Addendum [Furstenau 2021], jointly funded a program at Pacific Northwest National Laboratory (PNNL) to perform SCCI testing of these materials.

Since the inception of the NRC/EPRI SCCI testing program at PNNL, the Alloy 182 test matrix has evolved and grown as a result of not-before-seen Alloy 182 SCC initiation response. The primary areas of interest are currently stress exponent estimation, activation energy determination, dissolved hydrogen (DH) effects, and load cycling effects. Significant work has recently completed on stress exponent evaluation, temperature effects, and DH effects. This report focuses on providing up-to-date information on these topics.

The Alloy 600 tests support FOI determination for Alloy 690 SCCI times and also provide a basis of comparison for the Alloy 182 results. Yield stress (YS) and sub-YS Alloy 600 test results are covered in this report.

2.0 Experimental Setup

2.1 Test Method

As described in detail in a prior report [Toloczko 2017], the test method selected for this program was based on a review of known test methods conducted prior to the start of research. Both specimen type and the data provided by the test method were evaluated. Attributes that are highly desirable for stress corrosion crack (SCC) initiation testing include:

1. Efficient use of available material. SCCI measurements of welds are an important part of this program. Welds are limited in size, especially if the weld is a mockup of an actual plant component, such as a feedwater nozzle dissimilar metal weld.
2. Ability to control material condition. It should be possible to test the material in any desired thermomechanical condition, in particular, the level of applied deformation should be controllable because the amount of deformation has a substantial effect on SCCI time, and some variability of deformation level is expected in plant components.
3. Ability to control specimen surface condition. Plant components may have a range of surface conditions as a result of the component fabrication method. For instance, welds are often ground smooth, and this process produces a highly cold worked surface layer.
4. Ability to test at a precisely known and controlled stress. Correlation of initiation time to applied stress is an important part of this research effort. This is especially relevant to high temperature water testing where creep is known to occur in Ni-base alloys and will result in stress relaxation if passive loading is used.
5. Actively maintained environmental conditions. Water temperature and chemistry (especially impurity and DH content) affect SCC behavior.
6. Ability to test multiple specimens simultaneously. SCCI behavior can be highly variable for a given material, and thus multiple tests of each combination of material and test condition need to be conducted to evaluate the data statistically and more clearly interpret trends.
7. Ability to readily identify the initiation time.

Through tailored experimental approaches, tensile specimens are able to satisfy all the desired attributes simultaneously. Tensile specimens have often been used for SCCI testing, although typically as single specimen tests with the time to crack initiation approximated as the time to specimen failure rather than as the true time of crack initiation.

To accomplish the tests identified for the program, a multispecimen load line combined with in-situ measurement of time to crack initiation was designed to attain all the desired attributes. Up to 36 specimens can be tested simultaneously in one large test system, and in-situ measurement of crack initiation response is able to track the initiation behavior of multiple specimens simultaneously.

In-situ measurement of crack initiation is performed by the direct current potential drop (DCPD) method and has several desirable traits.

- In-situ detection of crack initiation allows for tests to be stopped at the early stages of crack initiation. This allows for observation of microstructures directly associated with the initiation response. This can have enormous value for identifying mechanisms controlling SCCI.

- The ability to track the initiation of multiple specimens, which allows for fewer test stops when conducting multispecimen tests. In contrast, if crack initiation is tracked by specimen failure, the test must be stopped and restarted for each specimen failure. For example, when a 12-specimen test is conducted using in-situ identification of crack initiation time, often two or more specimens initiate at similar times, and in most cases, no more than six test stops are needed during the course of the test. However, if time to failure is utilized for a 12-specimen test, then 12 test stops are likely to be required.
- The DCPD method allows for specimen strains to be precisely tracked, thus providing detailed information on not only the stress but also the level of strain applied to a specimen when specimens are brought up to test load. This makes it possible to evaluate the SCCI behavior of a material as a function of its complete stress and strain history.

2.2 Equipment

Test systems were designed and constructed for this program, and some test systems from other programs were made available for extended periods. These test systems are roughly identical with the exception of the autoclave size. Three sizes of autoclaves are being utilized for this research as shown in Figure 1, and the design of the systems was described in detail in previous reports [Toloczko 2017, Toloczko 2021b]. The small systems can test up to three specimens simultaneously, while the medium size test systems can test up to six specimens. The large test systems can test up to 36 specimens simultaneously.

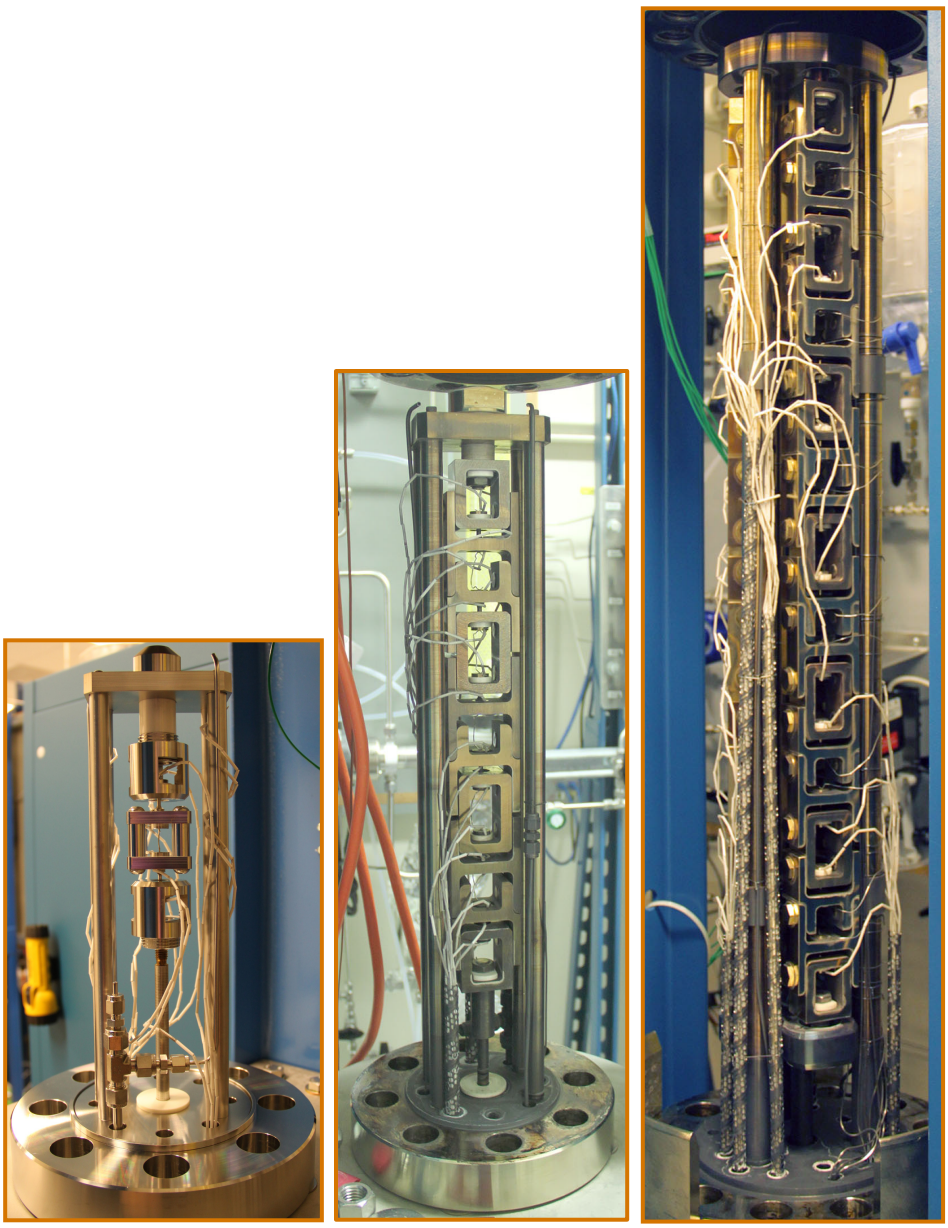

Figure 1. Load train for crack initiation testing as installed in PNNL's small, medium, and large autoclave systems. The interior heights are approximately 33, 60, and 100 cm, respectively.

The systems monitor, and in some cases, control key parameters, such as autoclave temperature, autoclave pressure, control load, and verification load to maintain specimen environmental stability. An example of the variability of some of these parameters is provided in Figure 2. Load is applied to the specimens as a combination of servo load and pull rod tare load. Servo load is very stable, exhibiting record-to-record variations of no more than +/- 0.1 kg. Verification load (called backup load in the plot) shows some long-term drift, and for this observation, the total span of the drift is no more than 0.3 kg. Tare load that is controlled by water pressure has a nominal value of 147 kg and is stable to within +/- 1.5 kg. This results in a total load variability of +/- 2 kg and represents a <0.5% variability applied load for the typical target test load of ~454 kg. Temperature is extremely stable with a variation within +/- 0.1°C.

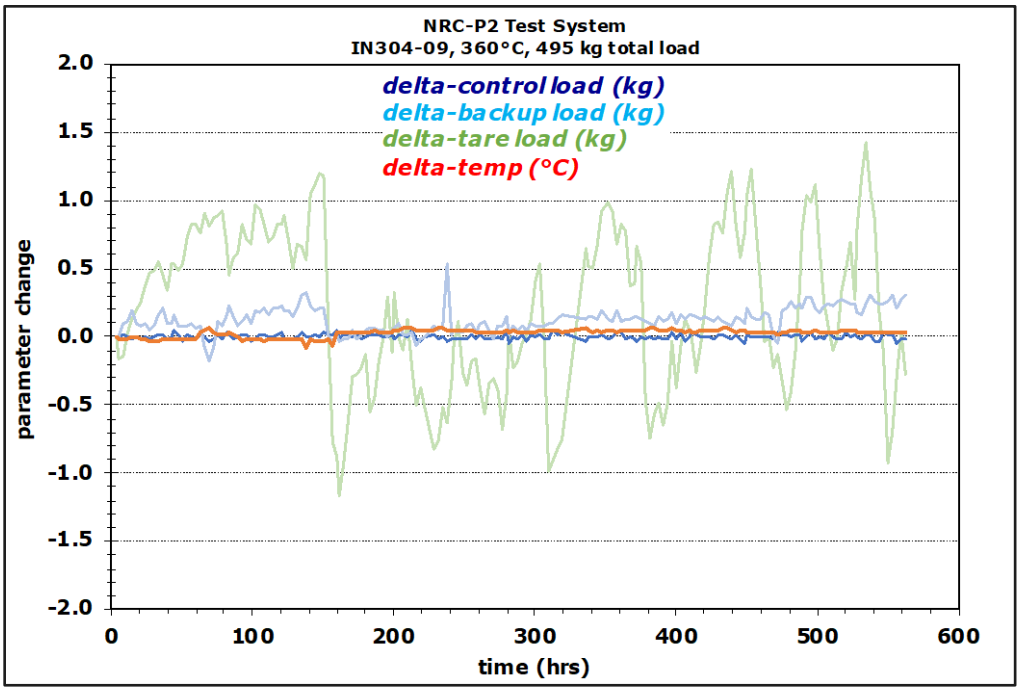

Figure 2. Servo load, verification load, pull rod tare load, and temperature variation for a PNNL high temperature water SCC test system over a period of ~575 hours.

2.3 Test System Improvements

Over the course of 10 years of test system usage, three aspects of the test systems have required improvement, namely the DCPD system for in-situ detection of SCC initiation, the high pressure pumps for the high pressure water loop, and the autoclave closure sealing process. The issues with the DCPD system were 1) low signal-to-noise ratio (SNR) in some of the systems, and 2) strong sensitivity to changes in laboratory environment, most likely temperature. Disassembly of the DCPD wiring in the problematic systems revealed incorrect assembly of the wiring that allowed for substantial crosstalk among the wiring and to earth ground. Rebuilding the wiring provided substantial improvements in SNR and reduced sensitivity to the laboratory environment. Further improvements in SNR were obtained through more careful grounding of shields and application of other electromagnetic interference (EMI) reduction techniques that had not been previously applied. Rewriting the DCPD hardware control algorithm to change how the nanovolt meter performs the DCPD measurements also resulted in a substantial improvement in SNR.

Another area of ongoing improvement is sealing the autoclave closure gasket on the large test systems. While all three size autoclaves have the same approach to gasket sealing, the large systems are more difficult to successfully seal at test start. An unsuccessful seal requires cooling the system, replacing the gasket, and reheating the test system, which consumes time and money. Through a combination of optimized bolt torque procedure and adjusting the gasket dimensions, the large autoclaves are typically successfully sealed on the first try.

2.4 Testing Protocol

The design of the SCC specimens is provided in Figure 3, while a sketch of a specimen showing idealized voltage measurement points is shown in Figure 4.

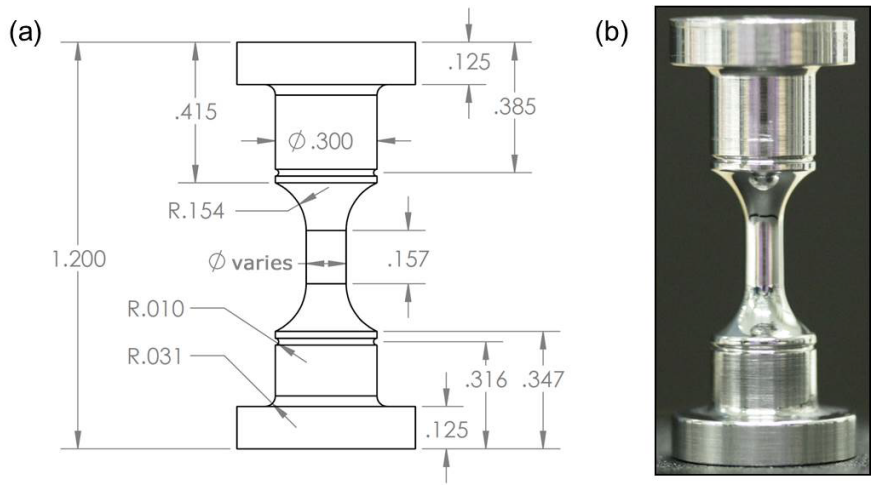

Figure 3. PNNL initiation specimen design with dimensions in Imperial units. Gauge diameter is selected based on material strength and can be varied from 0.108-0.177 in. (2.75-4.5 mm). Gauge length is 0.157 in. (4.0 mm). Overall height is 1.2 in. (30.5 mm).

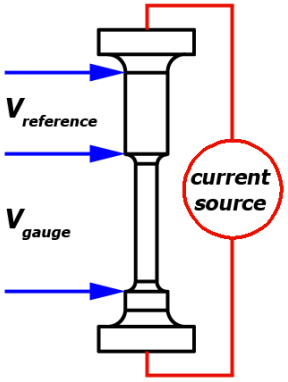

Figure 4. Sketch of the tensile specimen showing idealized DCPD measurement points.

Up to the point of crack initiation, the DCPD signal is affected largely by creep. For this reason, PNNL reports the DCPD response as a strain value. A formula for strain as a function of voltage starts first with the dependence of voltage on gauge dimensions:

$$V = \rho(L/A) \qquad \text{Equation 1}$$

where V is the measured voltage, ρ is the material resistivity, L is the distance between measurement points, and A is the cross-sectional area. Because plastic strain (including creep) is volume conservative, the relationship can be rewritten as:

$$V = (\rho/\nu)L^2 \qquad \text{Equation 2}$$

where ν is the volume of material between the voltage measurement points. By rearranging this equation to solve for L and inserting it into the equation for true strain [$\varepsilon = \ln(L/L_o)$], the strain as a function of voltage is obtained from the following formula:

$$\varepsilon_{referenced} = \frac{1}{2}\left[\ln\left(\frac{V_{gauge}}{V_{gauge_o}}\right) - \ln\left(\frac{V_{ref}}{V_{ref_o}}\right)\right]$$

Equation 3

where $\varepsilon_{referenced}$ is the resistivity corrected creep strain, and "gauge" and "ref" are measurements across the gauge section and reference region, respectively.

Due to the specimen test fixture obstructing the idealized voltage measurement points, the actual voltage pickup points are at slightly different locations than indicated in Figure 4. The deviation in voltage from idealized pickup points was assessed using finite element modeling, and a correction factor as a function of gauge diameter was determined. Further details on this DCPD measurement method can be found in another report [Bruemmer 2014].

All specimens are machined so that they reach their target testing stress at a load of 1000 lb (454 kg). This permits selection of any grouping of specimens for testing simultaneously through serial loading as described previously.

The gauge surfaces of all specimens are polished to a 1 µm or to a colloidal silica finish to facilitate identification of surface features and cracks both before and after a test. The surface finish was achieved by polishing the specimens in a lathe spinning at 200 rpm. In typical polishing fashion, the gauge surface was subjected to gradually finer polishing abrasives starting with SiC sandpaper and eventually switching to a polishing cloth with 6 µm, 1 µm diamond paste, and then colloidal silica compound. These abrasives were applied to the specimen using a thin stick that was moved systematically back and forth along the gauge by hand. Each grinding or polishing step normally requires ~30 seconds to 2 minutes while lubricant oil is dripped onto the tool whenever necessary. After each step, the specimen is rinsed in dish soap water, and then the gauge surface is checked using an optical stereoscope. Upon completion, the specimen is sonicated twice in dish soap water, once in 2% ethanol, and then dried. The effect of surface finish on SCCI is not within the scope of this study, but previous experience with Alloy 600 suggested no difference in initiation response for a polished or ground finish with this specimen type [Toloczko 2015, Zhai 2017]. PNNL testing has consistently shown that ground surfaces very slightly delay initiation time, as discussed previously.

The baseline environmental conditions for the tests are 360°C simulated pressurized water reactor (PWR) primary water with 1000 ppm of B, 2 ppm of Li, and a DH content of 25 cc/kg (corresponding to the Ni/NiO stability line at 360 °C). This temperature and DH content were selected as a mild test accelerant while still retaining the same stress corrosion mechanisms found in service. Water flow rate through the autoclave is maintained at ≥125 cc/min to ensure a consistent environment.

Within 48 hours of the test system reaching the target temperature, the specimens are brought up to their target load over a period of approximately two hours at a constant strain rate of approximately 10^{-5} mm/sec, analogous to conducting a tensile test. The stress versus strain evolution is continually monitored and plotted for each specimen during load-up, allowing production of a live stress versus strain plot. The stress is determined from the applied load and gauge diameter, while the strain is determined from DCPD, as previously described. The gauge diameter of each specimen is adjusted so that all specimens reach their YS at the same load. The loading is stopped when small plastic strains are observed in all specimens. Due to the inherent variability in the strength of materials as well as the precision with which the gauge diameter of a specimen can be machined, there is always some spread in the stress versus strain response of the specimens; some specimens yield sooner than others. The target plastic

strain is 0.2%, but when one or more specimens yield before others, loading is continued, and up to 3% plastic strain (depending on available work hardening capability of the material) is allowed in the specimens that yield early to give the other specimens a chance to reach 0.2% plastic strain. An example in which all specimens behave similarly during loading is provided in Figure 5, and an example of one specimen yielding earlier than others is provided in Figure 6. When test interruptions are performed to remove initiated specimens, the remaining specimens are brought back up to the original load using the same methods used during the start of a test. Specimens typically exhibit only linear response during reloading, but sometimes a specimen may exhibit a small amount of plastic strain.

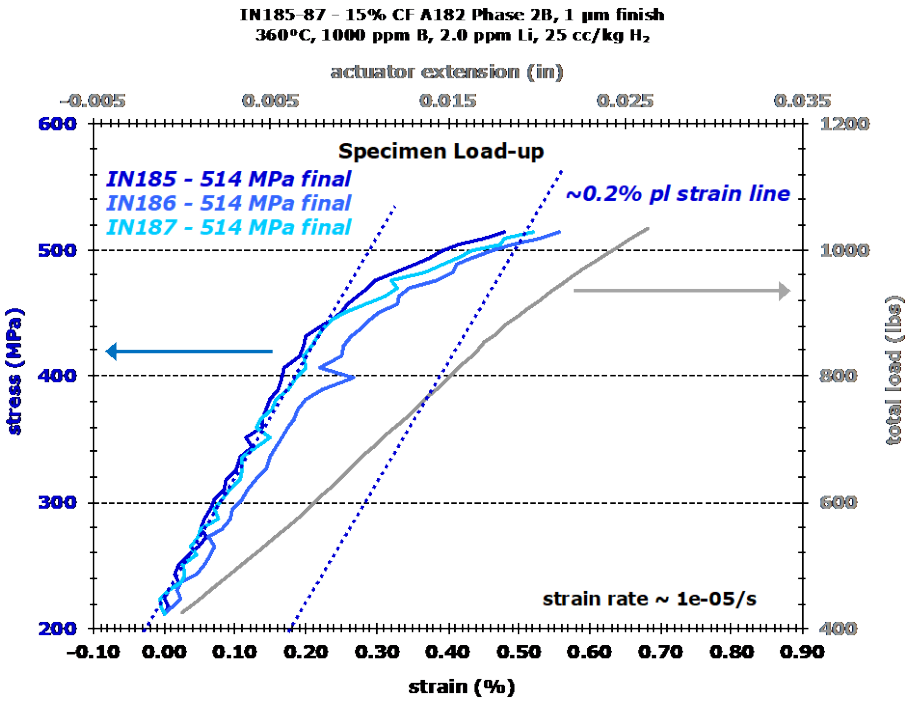

Figure 5. Example of a 3-specimen test being brought up to full load with all specimens exhibiting nearly identical stress versus strain responses.

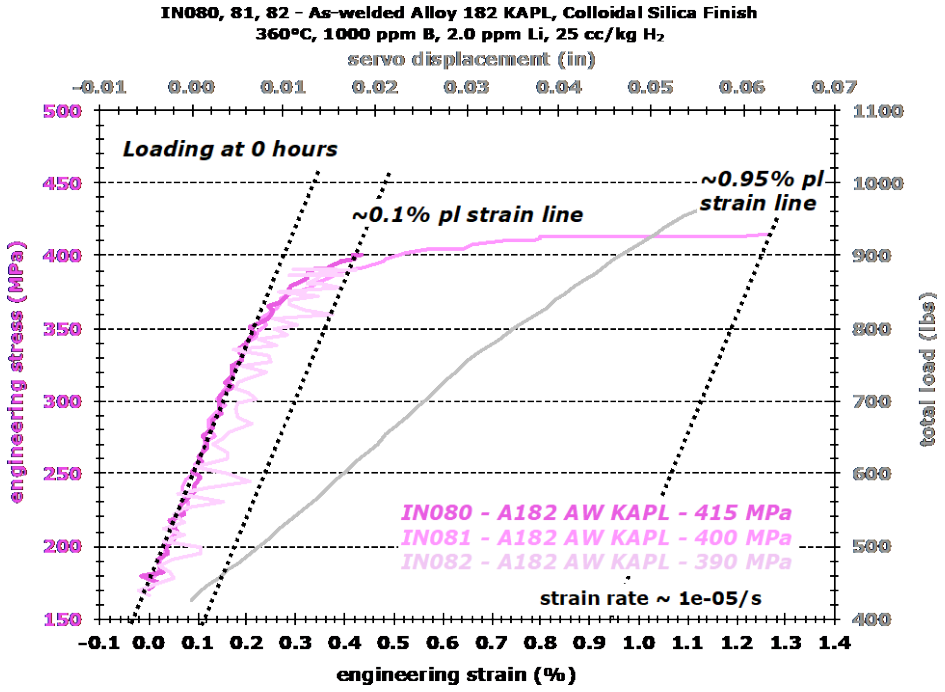

Figure 6. Example of a 3-specimen test being brought up to full load with one specimen yielding substantially earlier than the others.

During an SCCI test, the DCPD signal of each specimen is measured in the form of a creep strain. The strain response prior to initiation is typical of creep - a specimen exhibits a primary creep transient followed by a more steady-state response and eventually a change to positive curvature when a specimen initiates cracking. An example of specimen response exhibiting the typical stages of SCCI is provided in Figure 7.

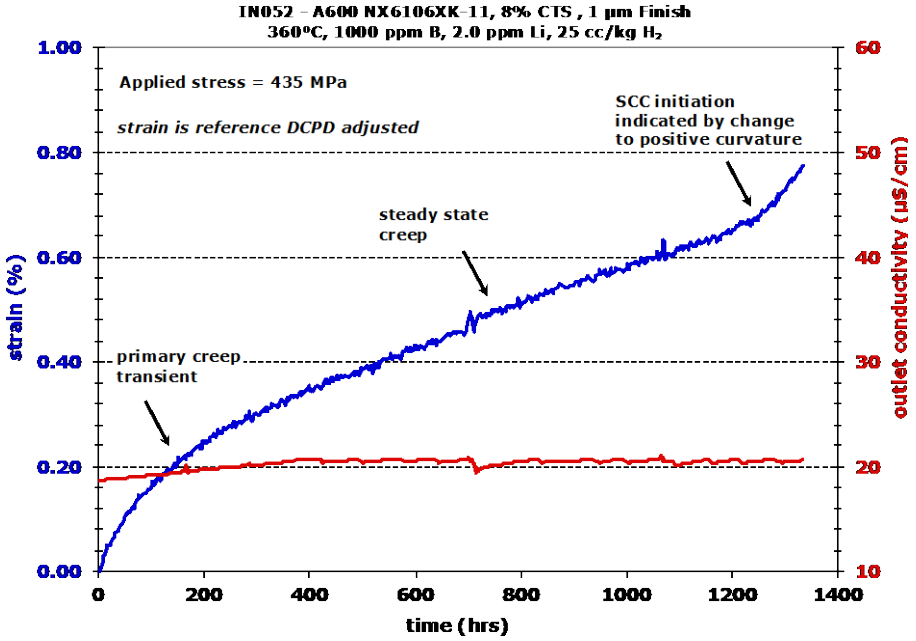

Figure 7. Typical SCCI test specimen behavior showing a primary creep transient, steady-state creep, and then the onset of SCCI.

2.5 Material Selection and Thermomechanical Condition

The Alloy 182 welds that were obtained are listed in Table 1. An additional weld mockup fabricated by Edison Welding Institute (EWI) was added to the test matrix during this reporting period. Compositions are listed in Table 2. Additional details of the materials are covered below.

Table 1. Alloy 182 materials used in this program.

Alloy 182	
NRC/PNNL Phase 2B DMW* Mockup	NRC/PNNL Flawtech DMW Mockup
Studsvik Buildup	KAPL U-Groove
Edison Welding Institute (EWI) U-Groove	

*DMW: Dissimilar metal weld

Table 2. Alloy 182 compositions from their weld wire CMTR.

Weldment	**Ni**	**Cr**	**Fe**	**C**	**Mn**	**Nb+ Ta**	**Si**	**Ti**	**Cu**	**S**	**P**	**Other**
KAPL	67.2	14.8	9.9	0.045	6.1	1.47	0.30	0.02	0.02	0.005	0.010	<0.5
Studsvik	70.3	13.9	6.6	0.043	7.1	1.47	0.26	0.01	0.04	0.003	0.010	<0.1
Phase 2B-L‡	69.4	14.1	6.0	0.032	8.2	1.65	0.27	0.28	0.06	0.001	0.003	<0.5
Phase 2B-U‡	67.6	14.6	7.3	0.058	7.8	1.80	0.29	0.43	0.05	0.001	0.003	<0.5
Flawtech	68.7	14.2	7.4	0.035	7.2	1.65	0.33	0.37	0.03	0.006	0.003	<0.5
EWI	74.0	14.5	3.6	0.030	5.4	1.82	0.57	0.02	0.04	0.004	0.001	NR
Specification	59.0 min.	13.0-17.0	10.0 max.	0.10 max.	5.0-9.5	1.0-2.5	1.0 max.	1.0 max.	0.50 max.	0.015 max.	0.030 max.	0.50 max.

‡: Two heats of weld wire were used.
NR: not reported

Alloy 182 is of particular importance to xLPR model validation, and the goal of the material acquisitions for this program was to obtain four representative mockup welds for SCCI testing. Two of the weldments are actual dissimilar metal reactor pressure vessel primary nozzle mockups. These weldments are the Phase 2B and Flawtech Alloy 182 mockups that were acquired by PNNL under other NRC programs. The third weldment, provided by EPRI, is a large bead-on-plate buildup of Alloy 182 that was previously used for SCC testing at Studsvik. This weld has exhibited high SCCGRs in tests performed on it by Studsvik. A fourth weldment was fabricated by Knolls Atomic Power Laboratory (KAPL), now named Naval Nuclear Laboratory. Etched optical images of a cross section of each of the Alloy 182 welds are presented in Figure 8 through Figure 11. The relative sizes of the welds to each other in these images is approximately correct. The Flawtech and Phase 2B welds are dissimilar metal nozzle welds made from ~36 cm diameter piping. SCCI testing is being performed on the fill region and not the butter. The KAPL weld is a groove weld in Alloy 600, and the Studsvik weld is a weld metal buildup that does not join two pieces of material. Further details of the materials are available in a previous report [Toloczko 2017].

A fifth Alloy 182 weld mockup made by Edison Welding Institute for another NRC program at PNNL [Toloczko 2020] was added to the test matrix in 2021. This is a 36 inch long U-groove mockup in Alloy 600 plate with dimensions shown in Figure 12.

Figure 8. Cross-section optical image of an etched 15% CF Flawtech Alloy 182 weld.

Figure 9. Cross-section optical image of an etched 15% CF KAPL Alloy 182 weld.

Figure 10. Cross-section optical image of an etched 15% CF Phase 2B Alloy 182 weld.

Figure 11. Cross-section optical image of an etched 15% CF Studsvik Alloy 182 weld.

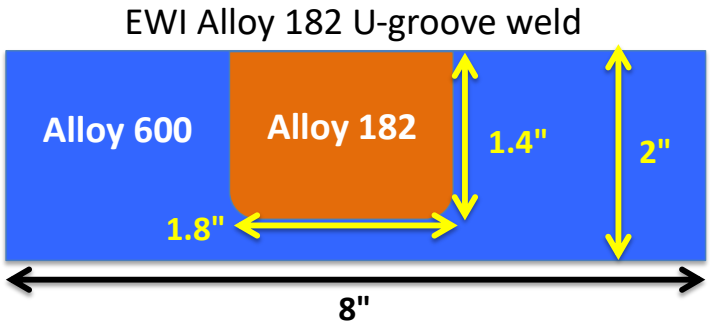

Figure 12. EWI Alloy 182 U-groove mockup sketch.

Most of the SCCI tests are being conducted on these materials in a 15% homogeneously cold forged (CF) condition. The selection of the appropriate level of cold work is an important aspect of this recommended test plan. It has been reported that highly damaged, cold work layers under very high stresses are relevant to plant SCCI conditions, but it is important to keep in mind that these microstructures and stresses fade to bulk values as a function of depth into a plant component. To best represent the varying damage level, an intermediate strength was chosen, namely 15% cold work appeared to be a reasonable intermediate level of damage. All welds were forged in the transverse direction with specimens aligned as shown in Figure 12, resulting in the crack initiation plane being along the most susceptible orientation relative to the cold forging and the weld microstructure.

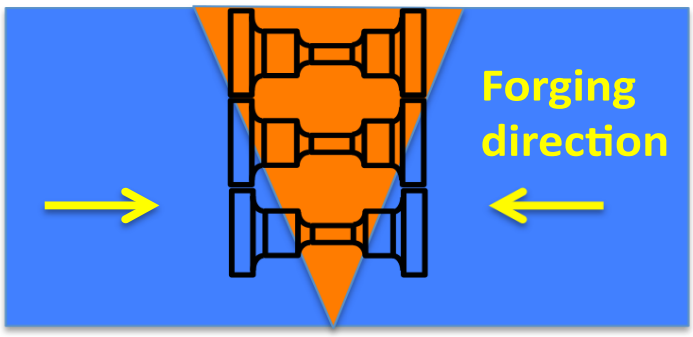

Figure 13. Orientation of forging direction and tensile specimens cut from weldments. The orange region represents a weld joint in cross section.

3.0 Alloy 182 Testing Status

3.1 Alloy 182 Tests Conducted at Yield Stress Loading

3.1.1 15% CF Alloy 182

SCCI tests were previously completed on the four 15% CF Alloy 182 welds at their YS in the baseline environment of 360°C water with the corrosion potential set to the Ni/NiO stability line. As shown in Table 3, 30 out of 36 specimens have undergone SCC initiation, and the remaining 6 specimens have run out to relatively long exposure times without SCCI. Average and median values for the entire set of specimens are 1453 hours and 736 hours (the exposure time of suspended specimens was assumed to be the initiation time of those specimens), respectively, while values for individual welds are listed in the table. While these values are commonly used in evaluating populations of data, due to the strong skew towards the low end of the SCCI time range, these statistical values provide only limited insight into the SCCI behavior of Alloy 182.

Table 3. SCC initiation times for nine each of four 15% CF A182 welds tested at YS. Mean, std. dev., and median of all specimens is 1453, 1858, and 736 hours, respectively.

KAPL	**YS (MPa)**	**t_{init} (h)**	**Studsvik**	**YS (MPa)**	**t_{init} (h)**
IN166	563	**≤30***	IN169	541	>5126
IN167	552	**≤30**	IN170	536	**30**
IN168	547	**113**	IN171	534	**2957**
IN194	581	**1635**	IN191	553	**83**
IN195	575	**1625**	IN192	559	**41**
IN196	567	**1642**	IN193	555	**41**
IN279	572	>5554†	IN233	532	**≤30**
IN280	566	>5554	IN234	529	**725**
IN281	576	>5554	IN235	532	**910**
Avg., S.D. Sample		***2415, 2541***	***Avg., S.D. Sample***		***1105, 1782***
Median		***1635***	***Median***		***83***
Phase 2B	**YS (MPa)**	**t_{init} (h)**	**Flawtech**	**YS (MPa)**	**t_{init} (h)**
IN185	514	**≤105**	IN188	518	**≤30**
IN186	514	>3173	IN189	518	**≤30**
IN187	514	**409**	IN190	518	**90**
IN197	500	**806**	IN200	528	**825**
IN198	506	**4964**	IN201	528	**746**
IN199	506	**2238**	IN202	528	**900**
IN216	462	**132**	IN221	525	**106**
IN217	467	>2971	IN222	525	**113**
IN218	467	**2908**	IN223	525	**79**
Avg., S.D. Sample		***1967, 1696***	***Avg., S.D. Sample***		***324, 378***
Median		***2238***	***Median***		***106***

* Gray highlight indicates no pretest examination of gauge surface. Red indicates that initiation is associated with an SEM-observable pre-existing defect. Blue indicates that initiation is not associated with any SEM-observable pre-existing defects.

† The ">" indicates not yet initiated.

** Statistical values are based on exposure time of initiated and non-initiated specimens.

SCCI testing was also conducted on another Alloy 182 weld named the EWI Alloy 182 weld. This is a U-groove weld in Alloy 600 plate that was fabricated for another NRC program. Eight out of nine specimens in a 15% CF condition tested at 360°C had initiation times below 30 hours, and the ninth specimen initiated in 75 hours. This weld has the lowest average initiation time of all the Alloy 182 welds tested at PNNL. SCCI times at 360°C for this weld are listed in Table 4.

Table 4. SCC initiation times for nine 15% CF Alloy 182 EWI welds tested at YS at 360°C.

EWI	YS (MPa)	t_{init} (h)
IN388	535	**<30**
IN389	537	**<30**
IN390	537	**<30**
IN391	536	**<30**
IN392	537	**<30**
IN393	544	**<30**
IN394	510	**<30**
IN395	513	**75**
IN396	513	**<30**
IN397	509	**<30**
IN398	510	**<30**
IN399	512	**<30**
Avg., S.D. Sample*		***34, 13***
Median		***30***

** Statistical values are based on exposure time of initiated and non-initiated specimens.

3.1.2 7.5% CF Alloy 182

Testing of 7.5% CF Alloy 182 at its YS is tentatively complete, with summary information presented in Table 5. Two of the four original Alloy 182 welds were tested with six specimens from each of the two welds. The shortest initiation time among the 12 specimens was 602 hours, while three specimens of each of the two welds reached >23,000 hours without initiation. The 602-hour initiation time for the KAPL Alloy 182 weld is ~20x higher than the shortest initiation time observed for these two welds in the 15% CF condition (~30 hours). The average initiation time of these two welds at their YS in the 15% CF condition is at least 1,760 hours, while for the 7.5% CF material, the average is at least 13,843 hours. This is a 7.9x longer SCCI time for 7.5% CF compared to 15% CF. These statistics indicate a substantial increase in SCCI resistance at 7.5% CF Alloy 182 compared to 15% CF. Specimen gauge surfaces have been documented by scanning electron microscopy (SEM) and summary images are being prepared.

Table 5. SCCI times for six each of two 7.5% CF Alloy 182 welds tested at YS. The combined mean, S.D., and median times are 13,843, 10,334, and 15,444 hours.

KAPL	YS (MPa)	t_{init} (h)	Studsvik	YS (MPa)	t_{init} (h)
IN236	471	**734**	IN227	452	7734*
IN237	472	**602**	IN228	440	7734*
IN238	473	**1025**	IN229	456	7734*
IN310	462	>23697†	IN313	442	>23154
IN311	463	>23697	IN314	442	>23154
IN312	463	>23697	IN315	445	>23154
Avg., S.D. Sample*		***12242, 12549***	***Avg., S.D. Sample.***		***15444, 8446***
Median		***12361***	***Median***		***15444***

* Specimens overloaded. Testing cannot be resumed on these.
† The ">" indicates not yet initiated.
** Statistical values are based on exposure time of initiated and non-initiated specimens.

3.1.3 As-Welded Alloy 182

SCCI testing of the 12 non-CW Alloy 182 specimens was terminated at 44,480 hours with no DCPD-indicated SCC initiations. The test plot is provided in Figure 13. All but two specimens exhibited typical non-referenced strain evolution that is a combination of resistivity increase and creep. Two specimens, namely the IN071 (Flawtech) and IN078 (Studsvik), exhibited strain jumps during the life of the test. IN071 exhibited multiple small strain jumps. The terminal exposure time of these specimens is 31x longer than the mean initiation time of the 15% CF material and 60x longer than the median initiation time.

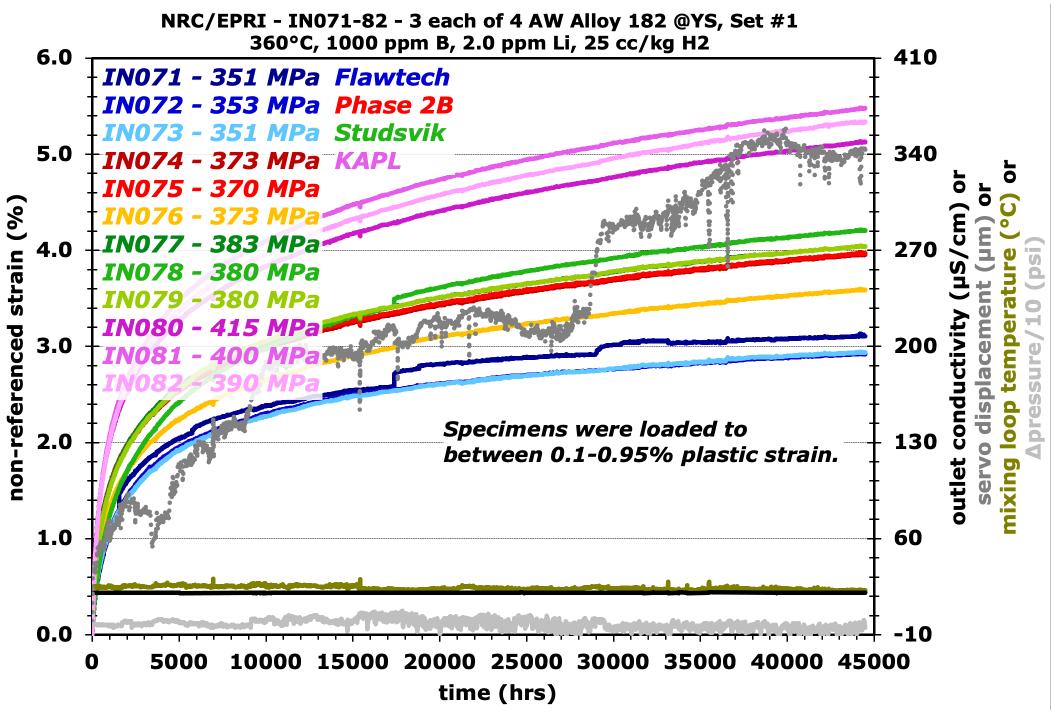

Figure 14. Non-referenced strain versus time plots for the as-welded Alloy 182 specimens.

Post-test gauge surface examinations are complete, and several specimens were found to have cracks or crack-like defects. A description of the observed defects is provided in Table 6. Out of the twelve specimens, two had obvious open cracks. Images of these two specimens are shown in Figures 14 and 15. Crack lengths varied from a 280 to 400 µm. These are relatively long cracks on the surface, and if the crack depth is roughly equivalent to the length on the surface, then it would be surprising that DCPD-based SCCI had not occurred. One possible explanation is that the crack depths could be shallow. Such behavior was observed for non-cold worked Alloy 600 [Zhai 2017]. One of the specimens with obvious open cracks – IN071 (Figure 14) – also exhibited multiple strain jumps during the SCCI test. However, the other specimen with open cracks – IN080 (Figure 15) – exhibited no strain jumps during the test. The other specimen that exhibited a strain jump – IN078 – had no obvious features on the surface of the specimen. Other specimens had isolated indications of enhanced grain boundary contrast that could be due to tight cracks or the presence of intergranular attack (IGA).

Table 6. Summary of post-test examination of the as-welded Alloy 182 specimens.

Specimen ID	YS (MPa)	Exposure time (h)	Strain Jump During Test?	SEM Observations of Gauge Surface
IN071 Flawtech	351	44,480*	Yes	Two **open** cracks, each ~400 µm on surface.
IN072 Flawtech	353	44,480	N	Two possible short cracks.
IN073 Flawtech	351	44,480	N	Two possible cracks, longest ~400 µm.
IN074 Phase 2B	373	44,480	N	One possible IGA.
IN075 Phase 2B	370	44,480	N	No features.
IN076 Phase 2B	373	44,480	N	Two possible IGA.
IN077 Studsvik	383	44,480	N	No features.
IN078 Studsvik	380	44,480	Yes	No features.
IN079 Studsvik	380	44,480	N	No features.
IN080 KAPL	415	44,480	N	Two **open** cracks, 280 & 360 µm on surface.
IN081 KAPL	400	44,480	N	No features.
IN082 KAPL	390	44,480	N	One possible crack, 260 µm on surface.

* None of these specimens exhibited DCPD-based SCCI.

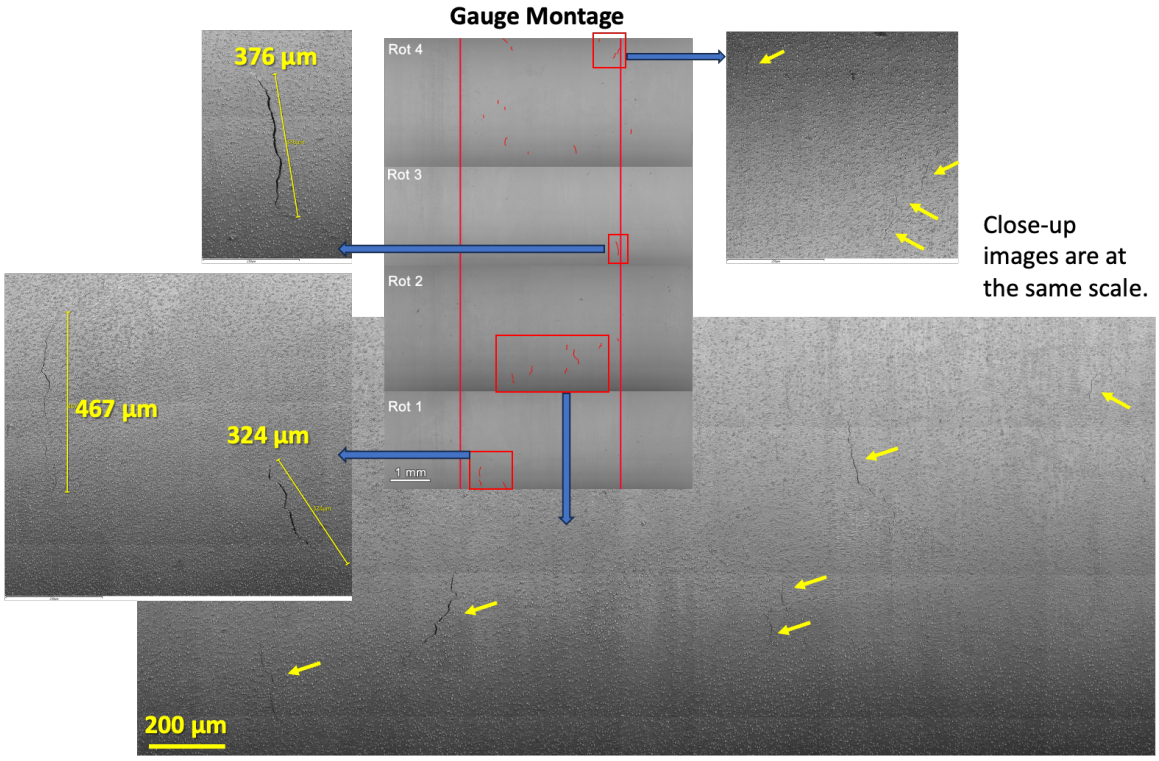

Figure 15. SEM-BSE images of the 15% CF Flawtech Alloy 182 IN071 specimen after 5.1 yrs.

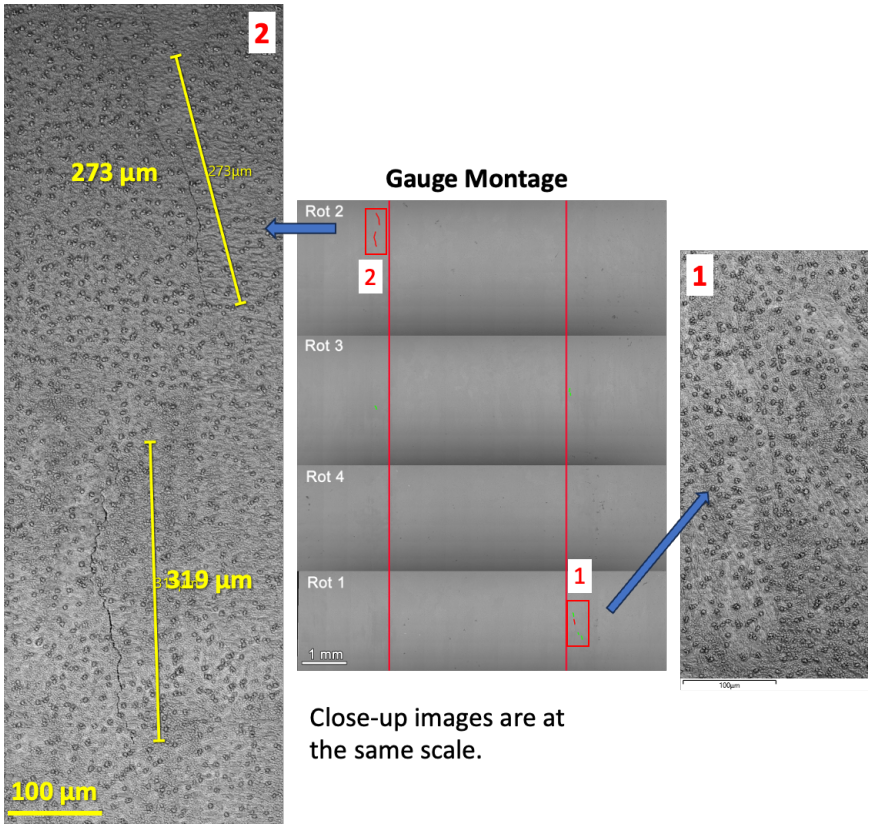

Figure 16. SEM-BSE images of the 15% CF KAPL Alloy 182 IN080 specimen after 5.1 yrs.

3.2 Alloy 182 Tests Conducted at Sub-Yield Stress Loading

SCCI tests conducted on two 15% CF Alloy 182 welds at 90% YS were covered in a previous report [Toloczko 2021b], and a summary table of initiation times is provided in Table 7. One specimen made from the KAPL Alloy 182 initiated at ~500 hours, while the remaining specimens initiated after 9,200 hours. The KAPL specimen that initiated at 500 hours had one of the lowest amounts of applied plastic strain during loading.

The ratio of the shortest initiation time at 100% YS (<30 hours) to the shortest initiation time at 90% YS (500 hours) suggests at least a ~17x increase in SCCI resistance at 90% YS. The average initiation time of all 12 specimens at 90% YS is at least 9,107 hours which is 5.2x longer than the average of these welds at their YS in the 15% CF condition (1,760 hours).

Table 7. SCC initiation times for six each of two 15% CF A182 welds tested at 90% YS. Mean, std. dev., and median of all specimens is 9107, 2772, and 9788 hours, respectively.

KAPL	Stress (MPa)	t_{init} (h)	Studsvik	Stress (MPa)	t_{init} (h)
IN251	505	**9205**	IN212	465	**10437**
IN252	505	**9312**	IN213	479	**10437**
IN253	505	**9284**	IN214	464	>10467†
IN254	513	**9178**	IN215	465	**10437**
IN255	513	**9312**	IN249	470	**10446**
IN256	513	**500**	IN250	466	**10264**
Avg., S.D. Sample		***7799, 3576***	***Avg., S.D. Sample***		***10415, 75***
Median		***9245***	***Median***		***10437***

† The ">" indicates not yet initiated.
** Statistical values are based on exposure time of initiated and non-initiated specimens.

3.3 Stress Dependence

3.3.1 SCCI of Highly Cold Forged Alloy 82

The U.S. Department of Energy – Nuclear Energy (DOE-NE) Light Water Reactor Sustainability (LWRS) project at PNNL was tasked to evaluate the SCCI behavior of Alloy 82 in KOH water chemistry [Zhai 2023]. As a result of that work, a batch of 30% CF Alloy 82 SCCI specimens were prepared and tested in beginning of cycle (BOC) KOH and LiOH water chemistry. As shown in Figure 16 for the LiOH water chemistry test and Figure 17 for the KOH water chemistry test, all the specimens exhibited extremely low SCCI times regardless of water chemistry. SCCI times were as low or lower than observed for the NRC/EPRI 15% CF Alloy 182.

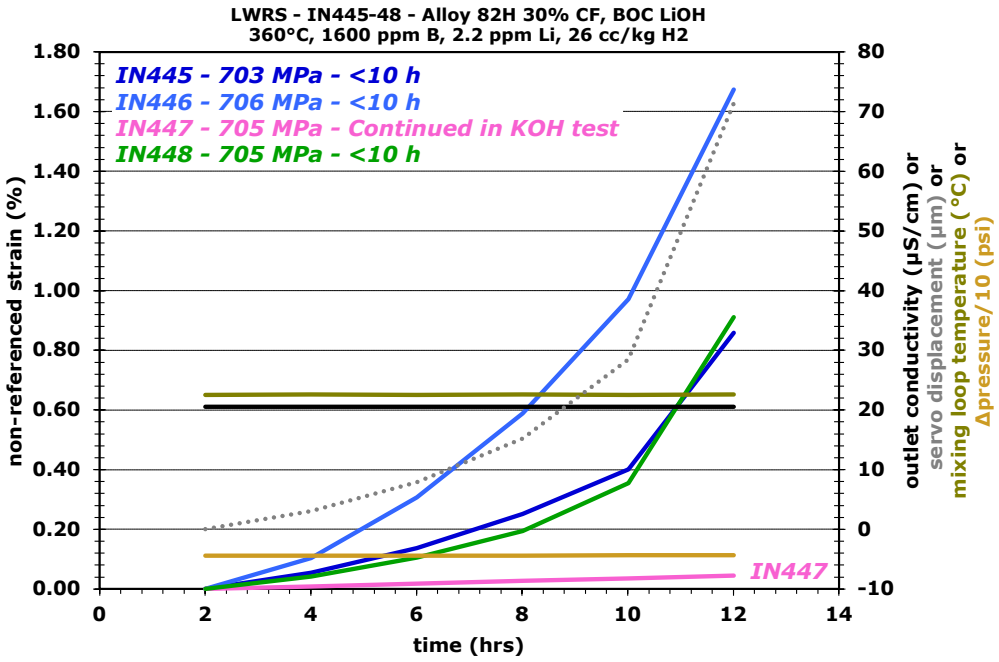

Figure 17. SCCI behavior of 30% CF Alloy 82 tested LiOH water chemistry for the DOE-NE LWRS program [Zhai 2023].

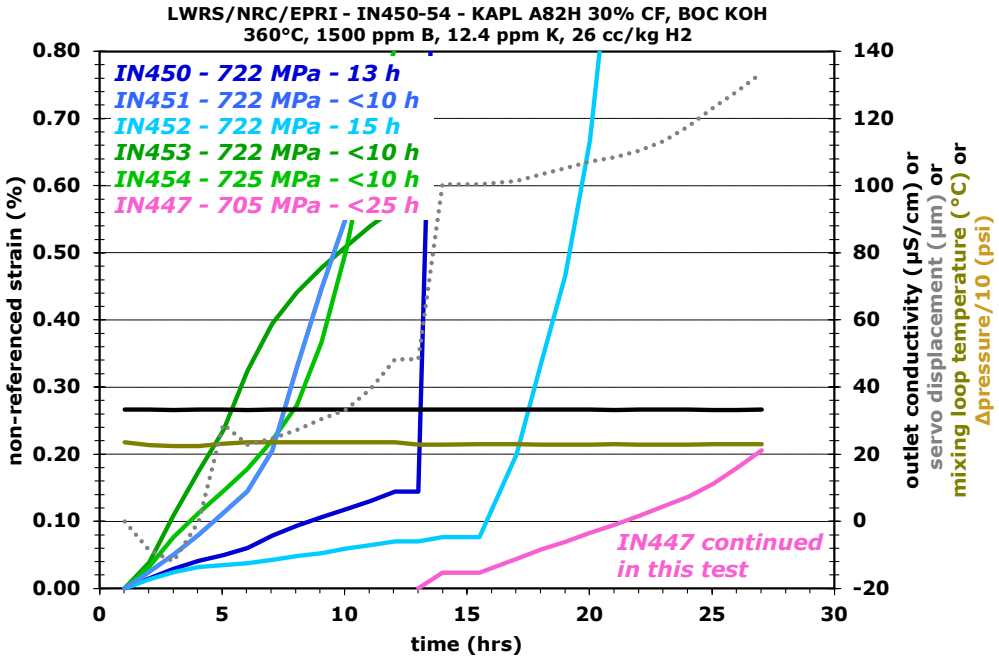

Figure 18. SCCI behavior of 30% CF Alloy 82 tested KOH water chemistry for the DOE-NE LWRS program [Zhai 2023].

Because the SCCI times of the 30% CF specimens were too low to discern any potential difference in SCCI behavior in KOH and LiOH water chemistry, another batch of specimens was prepared in a 15% CF condition and tested in the same way. The behavior of these specimens is provided in Figure 18 for LiOH water chemistry and Figure 19 for KOH water chemistry. As with the 30% CF specimens, the 15% CF specimens exhibited no sensitivity to water chemistry.

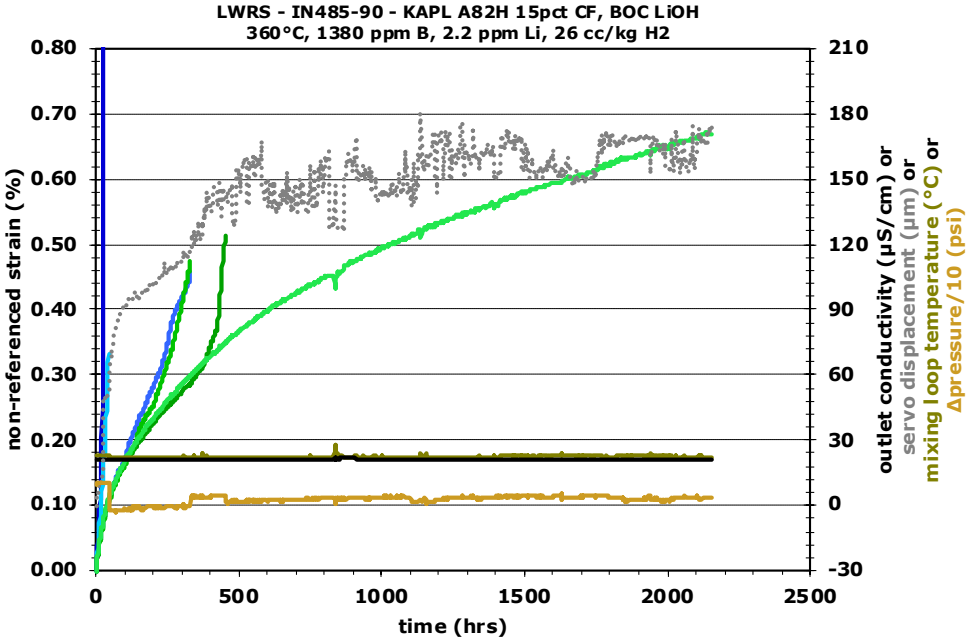

Figure 19. SCCI behavior of 15% CF Alloy 82 tested LiOH water chemistry for the DOE-NE LWRS program [Zhai 2023].

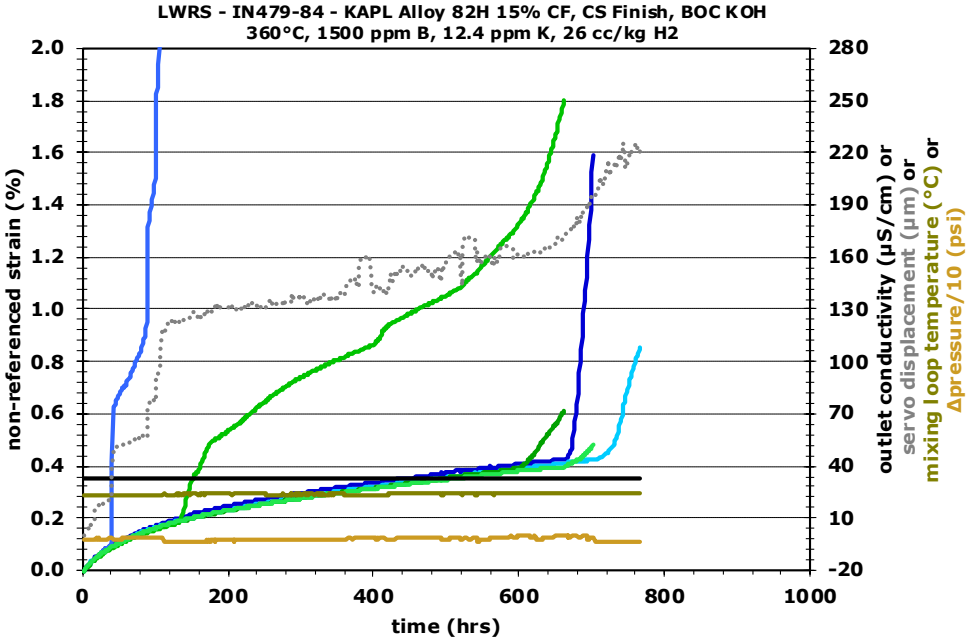

Figure 20. SCCI behavior of 15% CF Alloy 82 tested KOH water chemistry for the DOE-NE LWRS program [Zhai 2023].

The initiation times of these specimens were plotted together with the PNNL Alloy 182 data in Figure 20 and with the PNNL data and literature Alloy 182 data [Toloczko 2021b] in Figure 21. These data are adjusted to 325°C using an activation energy of 185 kJ/mole to compare the results to the literature data, which are also adjusted to 325°C using the same approach [Troyer 2015]. The 15% CF Alloy 82 data align well with the 15% CF Alloy 182, suggesting there is no significant difference in SCCI behavior between these materials in a cold forged condition. The 30% CF Alloy 82 data fit the overall trend of the data, further supporting that there is a large stress exponent for cold forged Alloy 182.

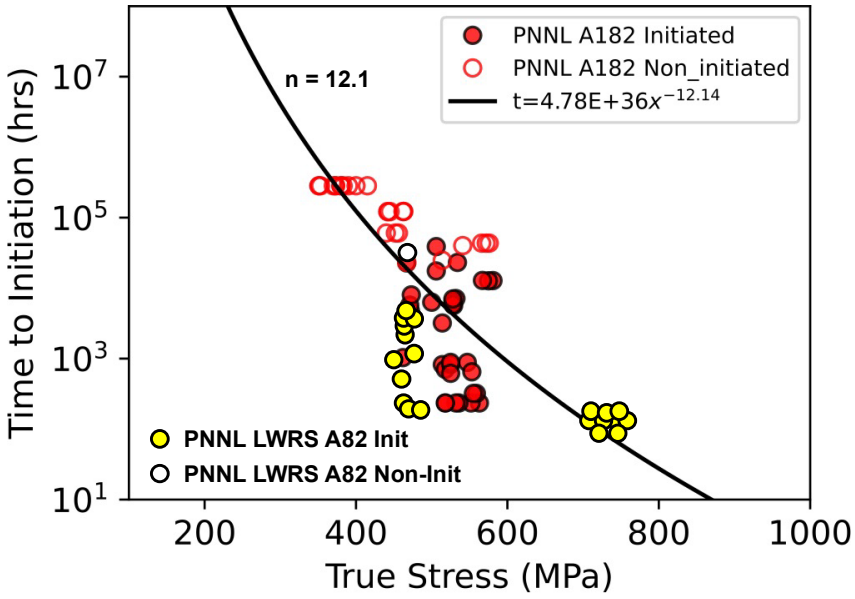

Figure 21. Stress exponent of cold forged NRC/EPRI Alloy 182 and LWRS Alloy 82 datasets combined.

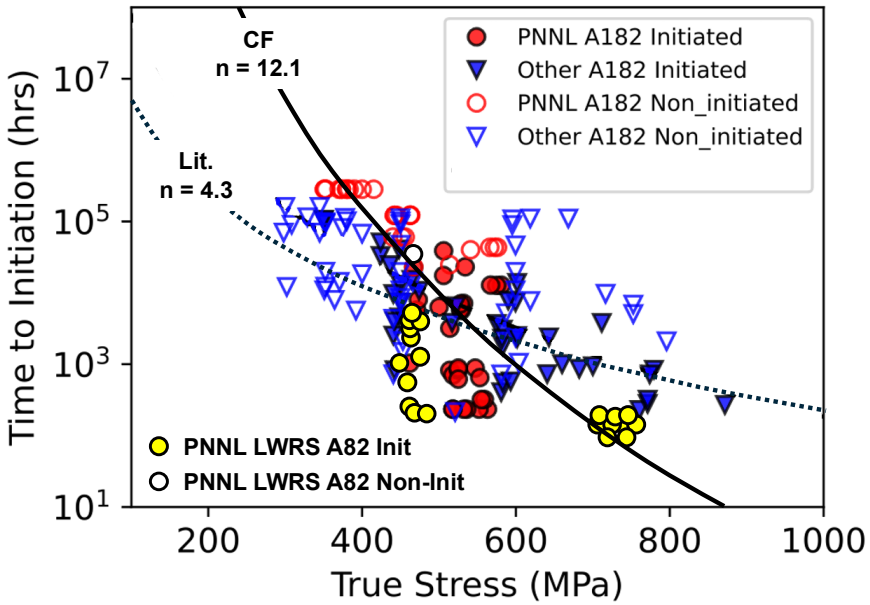

Figure 22. Stress exponent of cold forged NRC/EPRI Alloy 182 and LWRS Alloy 82 datasets combined and compared to the literature data on Alloy 182.

3.3.2 SCCI of Cold Tensile Strained Alloy 182

Two heats of the Alloy 182 material, namely the Studsvik and Phase 2B heats, were selected for SCCI testing in a cold tensile strained (CTS) condition. SCCI specimens with an oversize gauge diameter were machined and then CTS. Two strain levels were selected. 15% CTS was selected to allow for comparisons to specimens tested in the 15% CF condition, and 27% CTS was selected as the highest possible strain that could be attained while keeping a few percent strain below the point of mechanical instability (necking). Engineering strain values are used because this is directly comparable to the cold forging reduction calculation which is also calculated as a ratio to the original dimension.

Cold straining stress versus strain curves for the 15% CTS specimens are provided in Figures 22 and 23, while the curves for the 27% CTS specimens are provided in Figures 24 and 25. The obtained engineering strains and true stresses are listed in the figures. This activity went smoothly except that one of the specimens that was intended to reach 27% CTS failed early due to a pre-existing weld defect in the specimen. The obtained stress values were then used to tailor the gauge diameters of the specimens to allow testing all the 15% CTS specimens in one test system and the 27% CTS specimens in another test system.

After remachining the gauge diameters and polishing to a colloidal silica finish, the specimens were subjected to pretest SEM imaging of the specimen gauge surface. None of the 15% CTS specimens were observed to have any weld fabrication defects, but six of the twelve 27% CTS specimens were found to have defects. Some were quite small, as shown for example in Figure 26, while an example of a larger, approximately 100 µm long, defect is provided in Figure 27. The appearance of these is consistent with that seen in CF Alloy 182 specimens. Due to relatively low number of available specimens, the decision was made to SCCI test the defected specimens. These are marked with a “D” in the SCCI test plots.

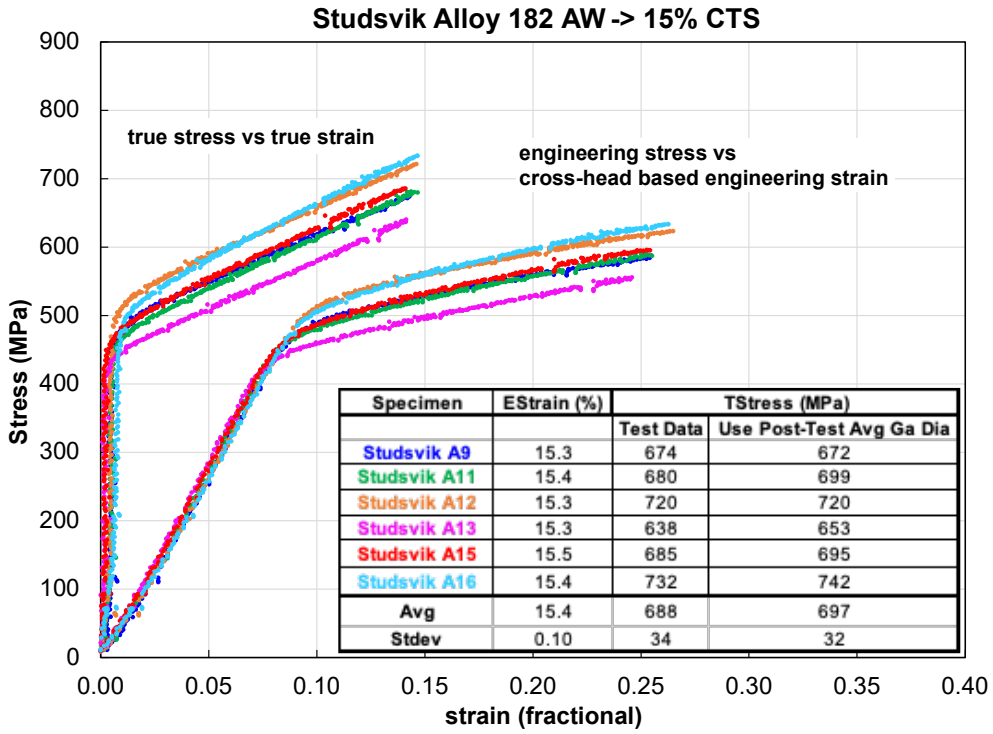

Specimen	EStrain (%)	TStress (MPa)	
		Test Data	Use Post-Test Avg Ga Dia
Studsvik A9	15.3	674	672
Studsvik A11	15.4	680	699
Studsvik A12	15.3	720	720
Studsvik A13	15.3	638	653
Studsvik A15	15.5	685	695
Studsvik A16	15.4	732	742
Avg	15.4	688	697
Stdev	0.10	34	32

Figure 23. Tensile straining of Studsvik Alloy 182 specimens to 15% CTS.

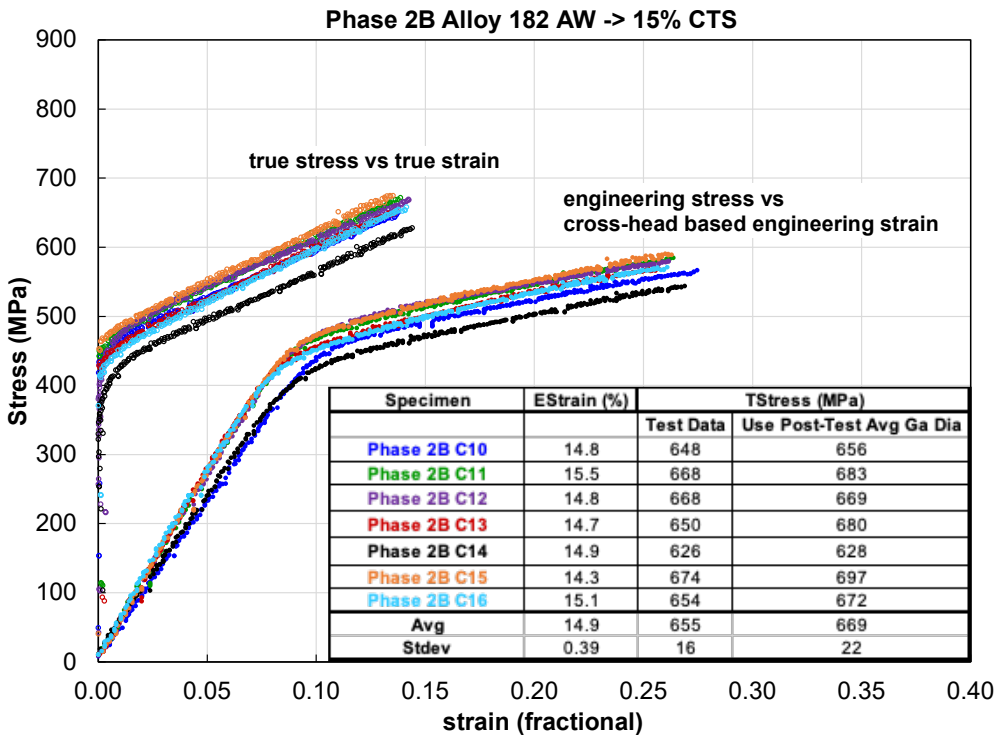

Specimen	EStrain (%)	TStress (MPa)	
		Test Data	Use Post-Test Avg Ga Dia
Phase 2B C10	14.8	648	656
Phase 2B C11	15.5	668	683
Phase 2B C12	14.8	668	669
Phase 2B C13	14.7	650	680
Phase 2B C14	14.9	626	628
Phase 2B C15	14.3	674	697
Phase 2B C16	15.1	654	672
Avg	14.9	655	669
Stdev	0.39	16	22

Figure 24. Tensile straining of Phase 2B Alloy 182 specimens to 15% CTS.

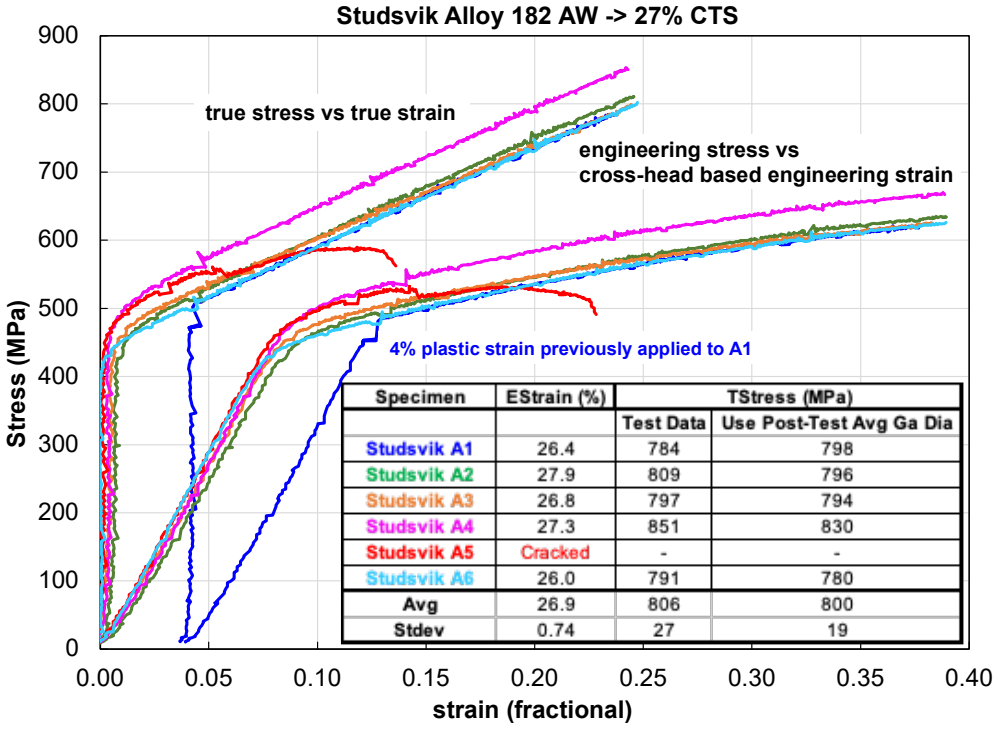

Specimen	EStrain (%)	TStress (MPa)	
		Test Data	Use Post-Test Avg Ga Dia
Studsvik A1	26.4	784	798
Studsvik A2	27.9	809	796
Studsvik A3	26.8	797	794
Studsvik A4	27.3	851	830
Studsvik A5	Cracked	-	-
Studsvik A6	26.0	791	780
Avg	26.9	806	800
Stdev	0.74	27	19

Figure 25. Tensile straining of Studsvik Alloy 182 specimens to 27% CTS. One specimen failed prior to reaching the target strain level.

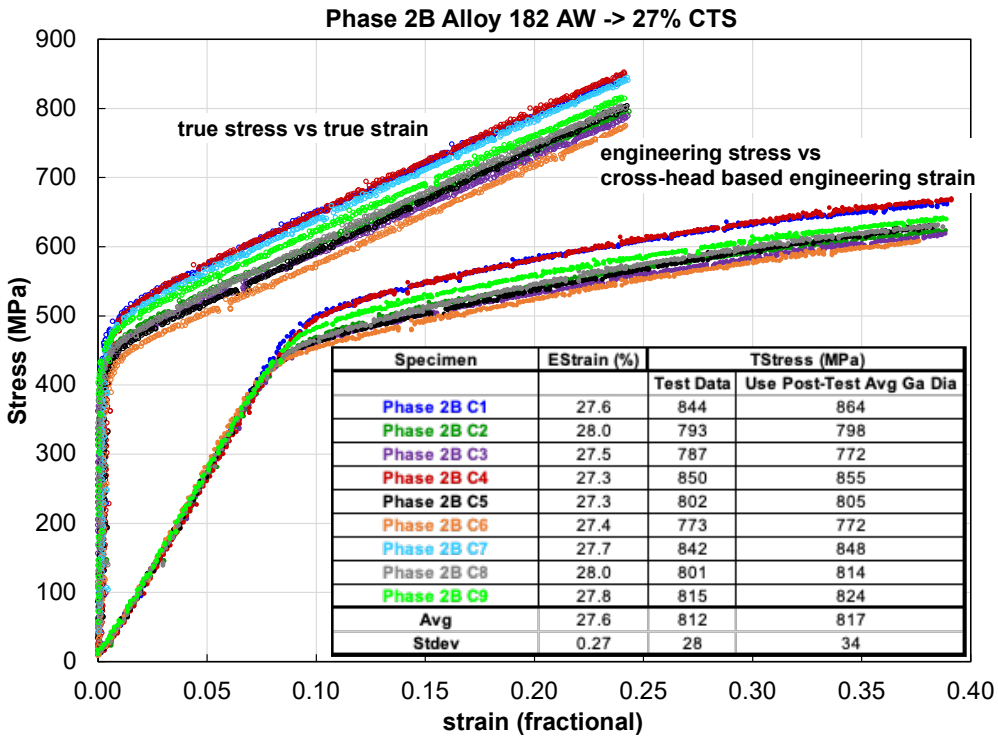

Specimen	EStrain (%)	TStress (MPa)	
		Test Data	Use Post-Test Avg Ga Dia
Phase 2B C1	27.6	844	864
Phase 2B C2	28.0	793	798
Phase 2B C3	27.5	787	772
Phase 2B C4	27.3	850	855
Phase 2B C5	27.3	802	805
Phase 2B C6	27.4	773	772
Phase 2B C7	27.7	842	848
Phase 2B C8	28.0	801	814
Phase 2B C9	27.8	815	824
Avg	27.6	812	817
Stdev	0.27	28	34

Figure 26. Tensile straining of Phase 2B Alloy 182 specimens to 27% CTS.

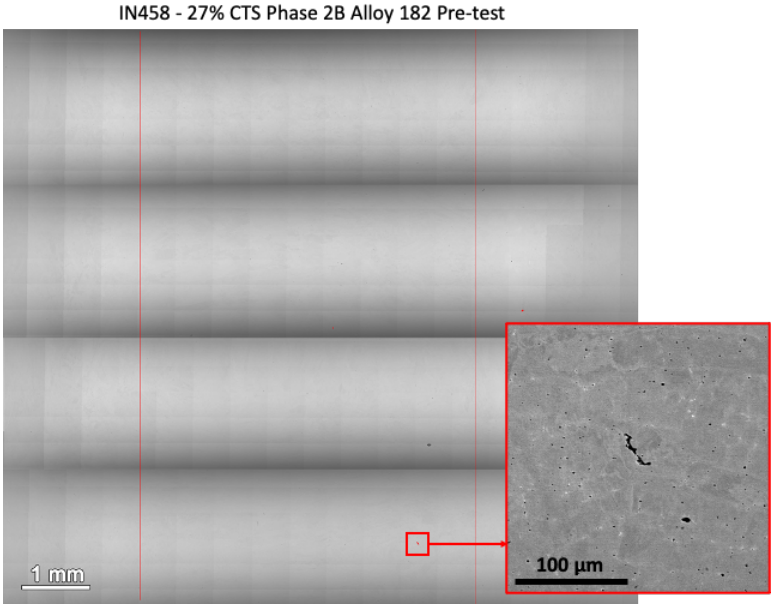

Figure 27. Example of a weld fabrication defect found on the surface of the IN458 27% CTS Phase 2B Alloy 182 specimen.

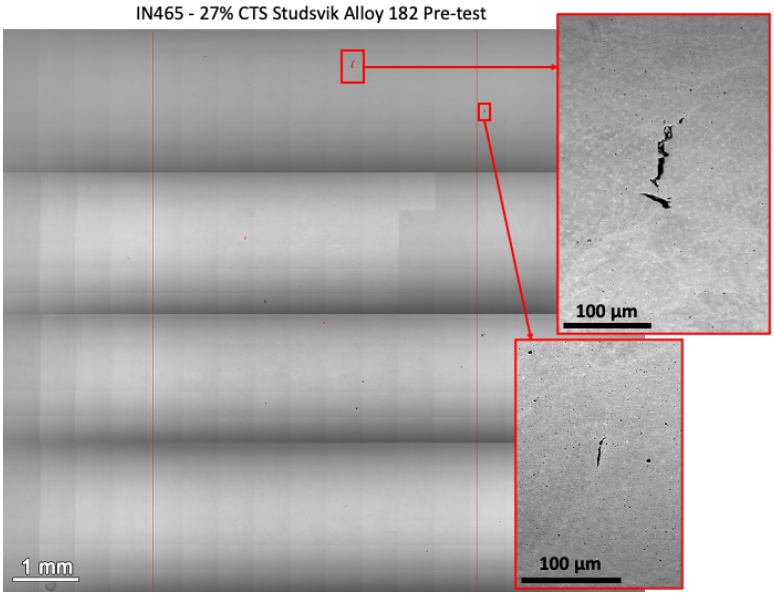

Figure 28. Example of a weld fabrication defect found on the surface of the IN465 27% CTS Studsvik Alloy 182 specimen.

Specimen load-up curves are provided in Figures 28 and 29 for the 15% CTS specimens and Figures 30 and 31 for the 27% CTS specimens. A wider range of attained load-up plastic strain was obtained for all these specimens. In some cases, load-up was stopped earlier than desired to try to avoid failure of a higher plastic strain specimen. The stress levels attained for the 15% CTS specimens are in the same range as the 15% CF specimens. The stress levels attained for the 27% CTS specimens were only 20-30 MPa higher than the 15% CTS specimens.

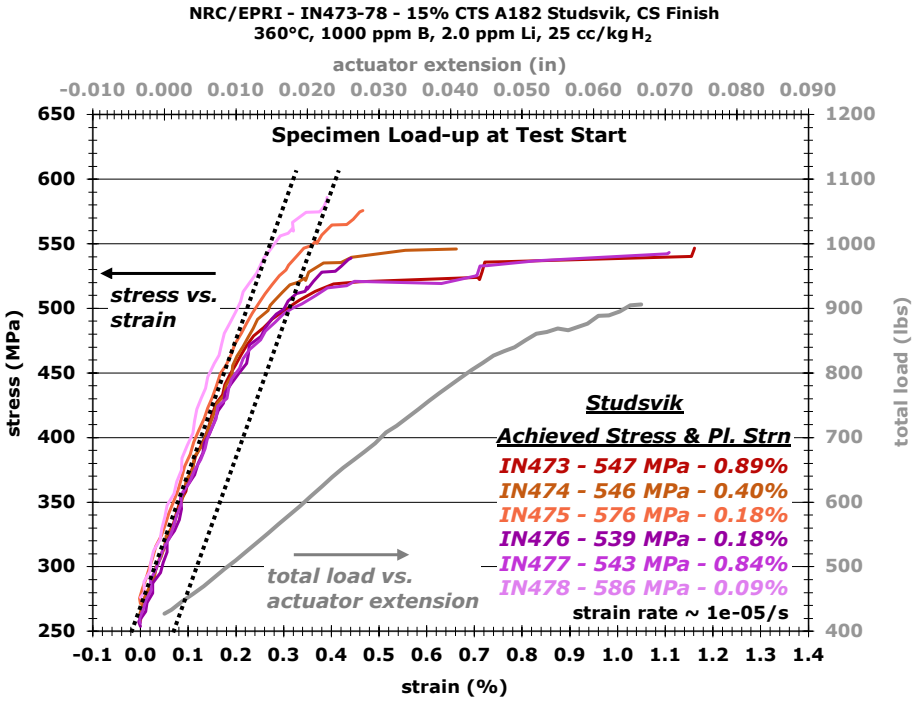

Figure 29. 15% CTS Studsvik specimen load-up stress versus strain curves.

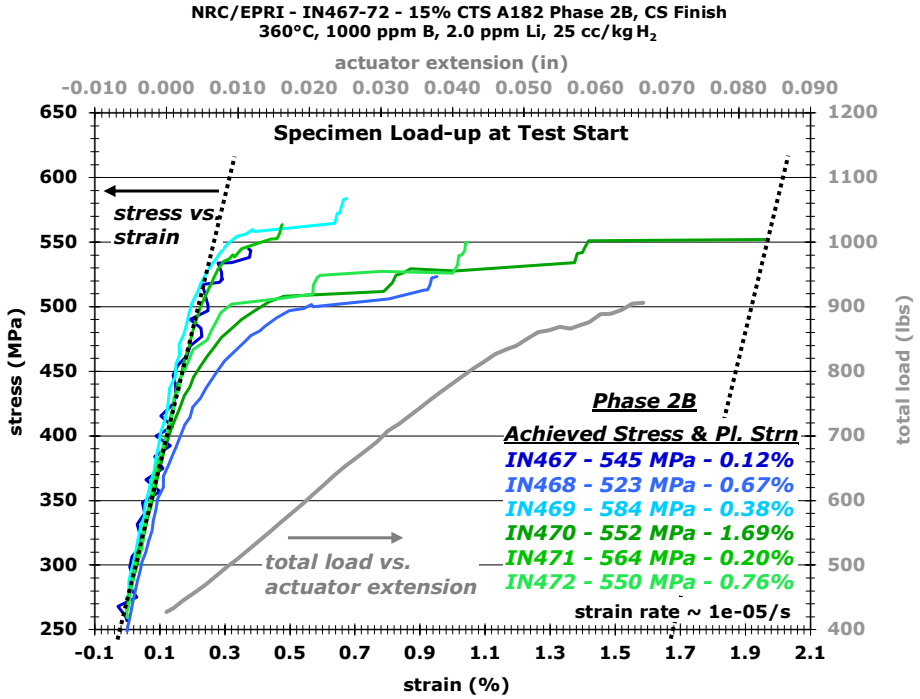

Figure 30. 15% CTS Phase 2B specimen load-up stress versus strain curves.

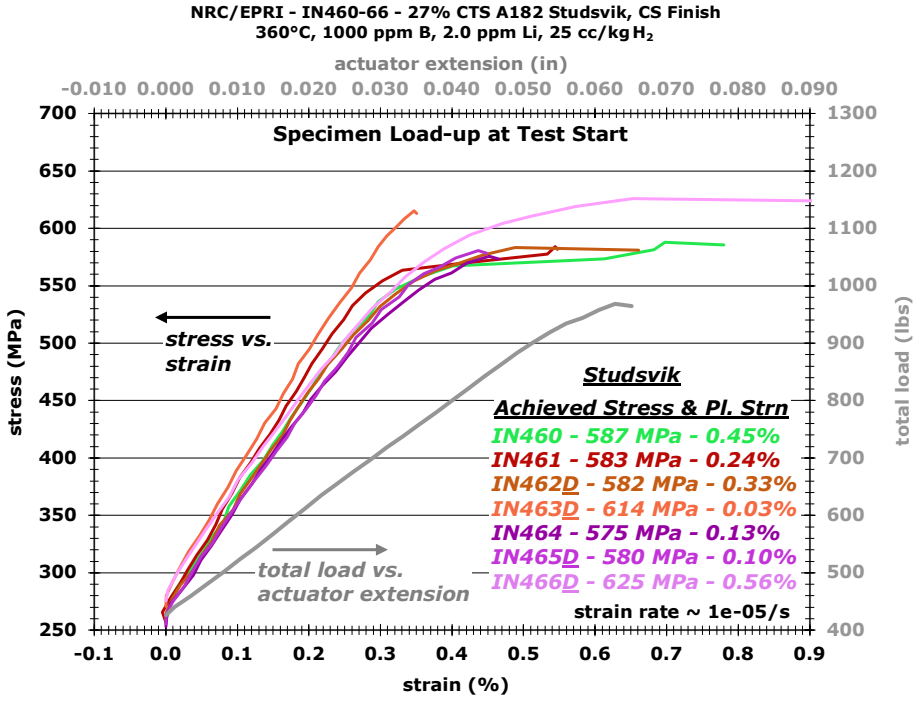

Figure 31. 27% CTS Studsvik specimen load-up stress versus strain curves.

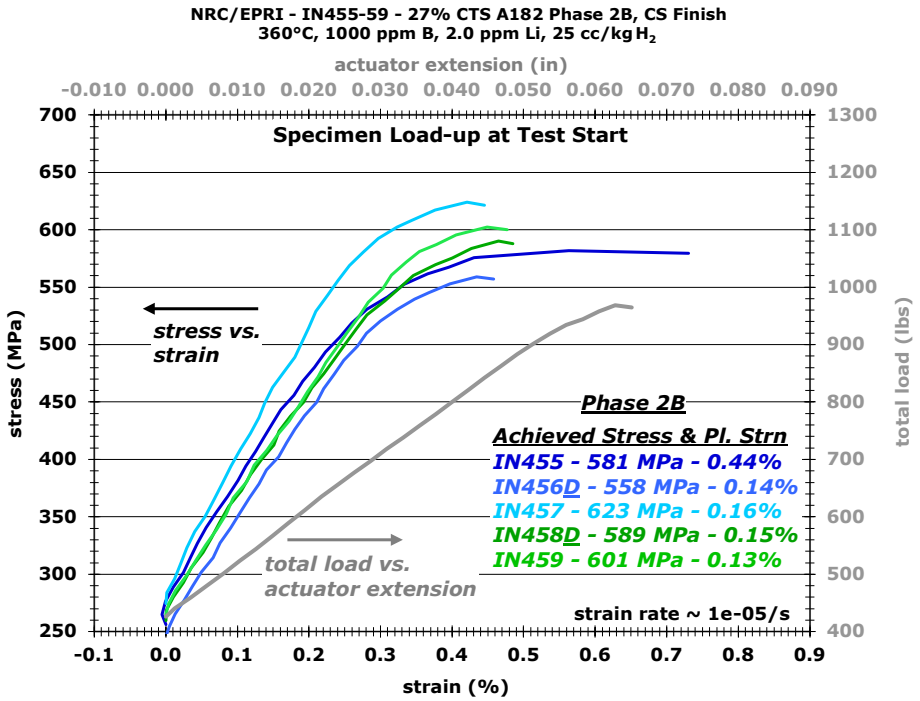

Figure 32. 27% CTS Phase 2B specimen load-up stress versus strain curves.

The constant load non-referenced strain plot for the 15% CTS specimens is provided in Figure 32. This ongoing test has reached 17,208 hours with no failed specimens. However, at approximately 3,000 hours, the Phase 2B IN468 specimen exhibited an approximately 0.5% strain jump, which can be better seen in Figure 33. Such strain jumps are typically attributed to a crack forming in a specimen, possibly due to crack coalescence.

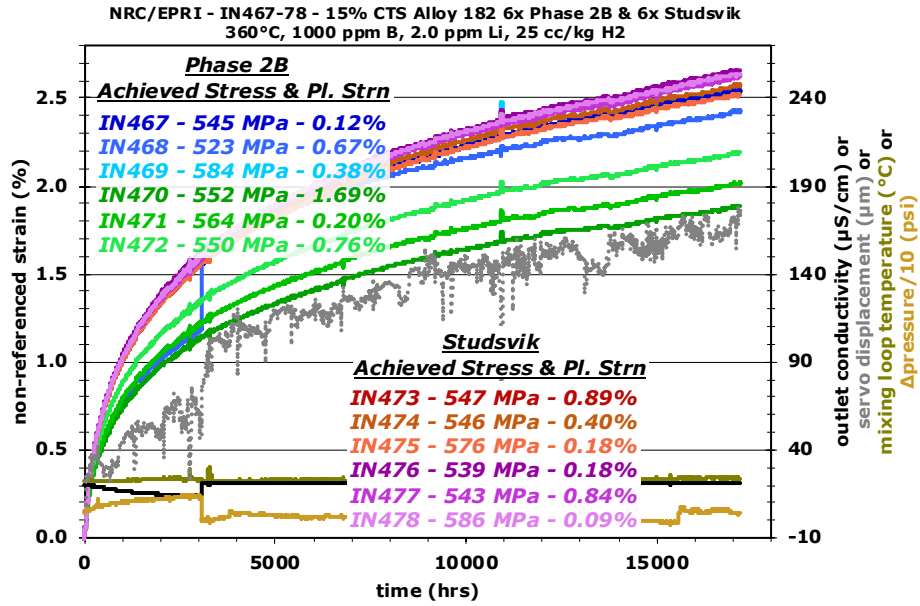

Figure 33. SCCI behavior of the 15% CTS Studsvik and Phase 2B Alloy 182 specimens. This test is ongoing.

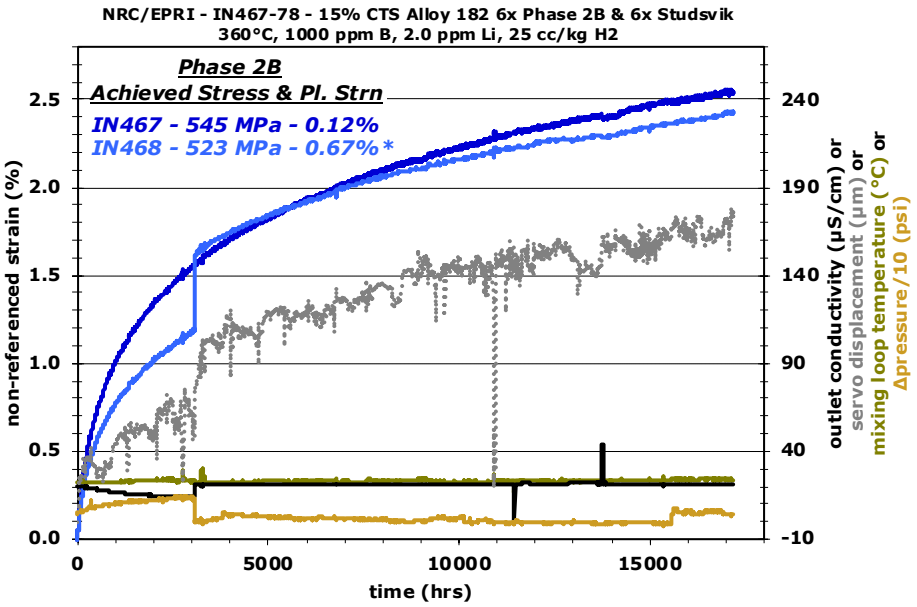

Figure 34. SCCI behavior of the 15% CTS Phase 2B Alloy 182 IN468 specimen showing that it exhibited a strain jump at approximately 3000 hours.

The constant load, non-referenced SCCI exposure plot for the 27% CTS Studsvik specimens is provided in Figure 34, while the 27% CTS Phase 2B specimens are shown in Figure 35. Five of the twelve specimens initiated within 500 hours while the remainder have reached 11,324 hours without failure. Four out of the five initiated specimens have weld fabrication defects in the gauge or fillet surface, but notably two of the non-initiated specimens also have weld fabrication defects. Therefore, it is unclear if weld fabrication defects contributed to SCCI behavior. Regardless of the weld fabrication defects, these 27% CTS specimens with test stresses higher than 15% CF material are much more resistant to SCCI than the 30% CF material.

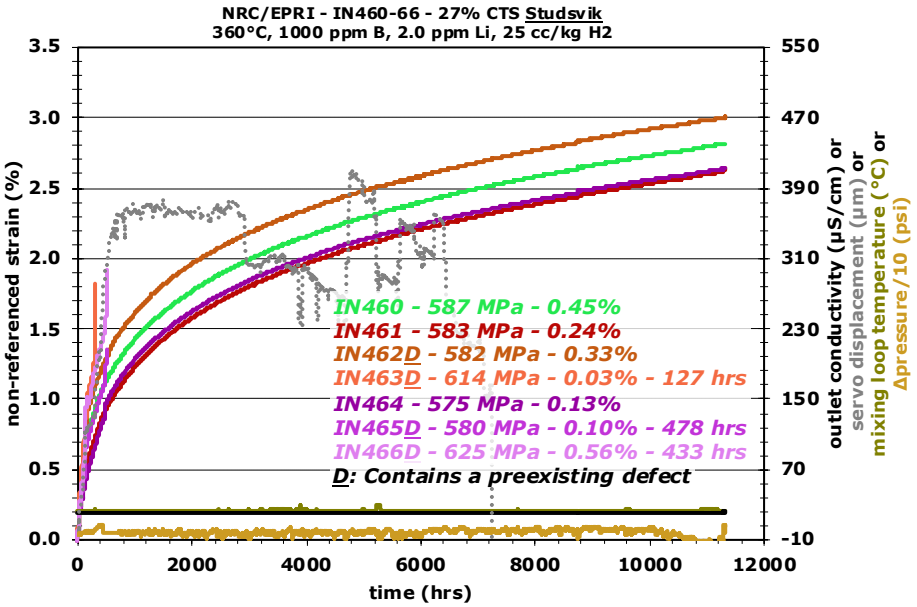

Figure 35. SCCI behavior of the 27% CTS Studsvik Alloy 182 specimens.

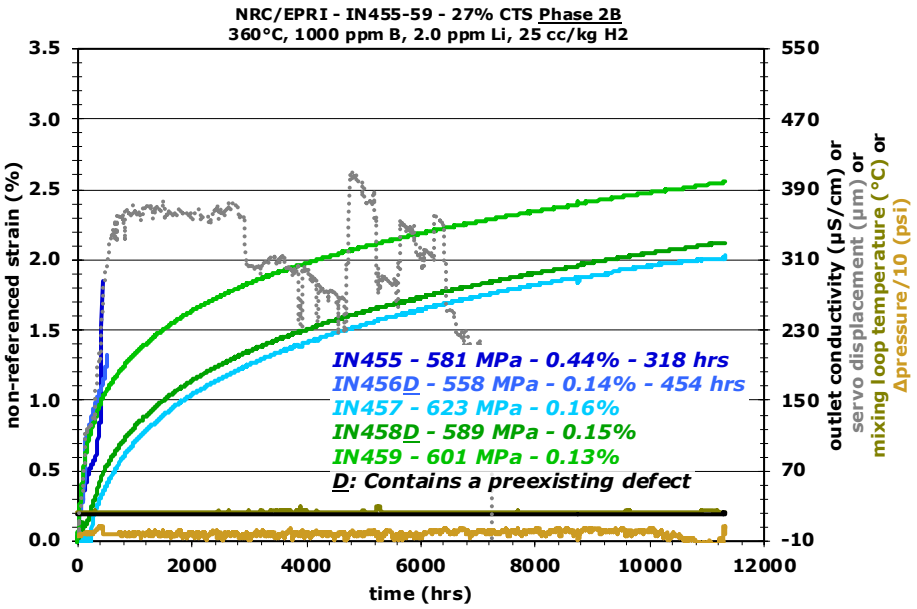

Figure 36. SCCI behavior of the 27% CTS Phase 2B Alloy 182 specimens.

3.3.3 Stress Dependence Discussion

The SCCI times of the non-initiated and initiated CTS specimens are plotted alongside all the other PNNL Alloy 182 and 82 SCCI data and the literature Alloy 182 data in Figure 36. None of the twelve 15% CTS Alloy 182 specimens have initiated and, to date, have longer initiation times than the 15% CF Alloy 182 data. Seven out of the twelve 27% CTS Alloy 182 specimens also have not initiated and have initiation times, to date, that are at the top of the distribution in their stress range. The PNNL cold tensile strain results are better aligned to the literature data on tensile strained and biaxial strained data than the PNNL CF data. The initiated CTS specimens sit on the literature trend line for tensile strained material, and like the literature data, there is an abundance of non-initiated specimens.

The strong difference in SCCI behavior between tensile strained and CF Alloy 182 highlights the complexity of determining a representative stress exponent for SCCI. It has been noted by French researchers [Berge 1997, Le Hong 1999, Scott 2007] that SCCI much more readily occurs in Alloy 182 that has undergone a strain reversal, i.e., first strained in compression, and then strained and exposed in tension. The data provided here generally fit that assessment with purely tensile strained material exhibiting much greater SCCI resistance than CF Alloy 182.

However, there are other unexpected features in the behavior of Alloy 182, in particular, non-CW Alloy 182 exhibits excellent SCCI resistance. Three specimens each of four different heats of Alloy 182 did not exhibit SCCI during 5.1 years of testing at the YS of the material. This behavior is in contrast to non-CW Alloy 600 that readily exhibits SCCI. Non-CW Alloy 600 SCCI tested at PNNL for the DOE-NE LWRS Program often exhibited SCCI in less than one year [Zhai 2017]. A compilation of literature Alloy 600 SCCI data prepared for the NRC/EPRI SCCI testing program [Toloczko 2021a] shows similar behavior with Alloy 600 tested at 300 MPa having an initiation time of approximately 2 years at 360°C when using Morton's Alloy 600 SCCI activation energy of 103 kJ/mol [Morton 2001]. The difference in SCCI behavior of Alloy 600 and Alloy 182 could be due to several factors. Compositionally, the two materials have similar Cr, Si, Fe, and C levels. However, Alloy 600 has less than 1 wt% Mn and is free of Nb and Ta, while Alloy 182 typically has 7 wt% Mn and a combined Nb+Ta content of 1.5 wt%, all at the

expense of Ni content. These are non-trivial differences in alloy composition. Grain morphology between Alloy 182 and Alloy 600 are also significantly different. Alloy 182 has a typical weld metal solidification grain boundary structure consisting of cylindrical shaped grains with highly crenulated boundaries and diameters of the order of 50-300 μm and lengths ranging from a few hundred micrometers to approximately 3 mm. Alloy 600 typically has an equiaxed grain structure with flat boundaries and a grain size of the order of 25-500 μm. Alloy 182 solidification grain boundaries are typically decorated with Nb carbides whereas mill annealed Alloy 600 (studied in this project) typically has a small number of grain boundary Cr carbides. Finally, Alloy 182 typically has a YS of approximately 375 MPa whereas Alloy 600 is typically 300 MPa. While these differences exist, none readily explain the difference in SCCI behavior between the two materials.

Operating experience has revealed that Alloy 182 in nuclear power plants may be highly susceptible to SCCI in certain conditions. The SCCI data provided here suggests that SCCI of Alloy 182 components in plants is much more likely to occur at locations where the component surface had been exposed to a complex mode of deformation.

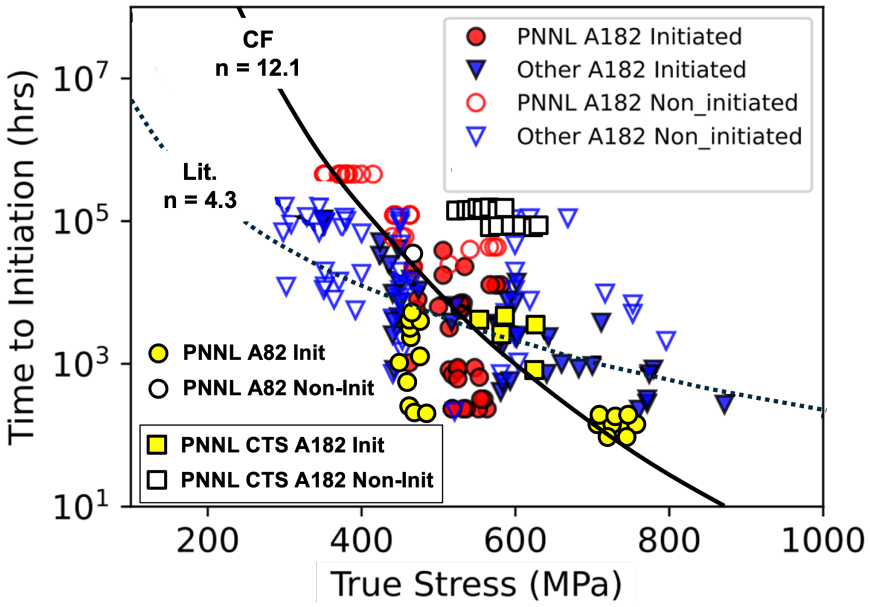

Figure 37. All PNNL Alloy 182 and Alloy 82 SCCI data obtained at 360°C. Data are corrected to 325°C to allow comparing to literature data.

3.4 Effects of Dissolved Hydrogen Content

This is a test of specimens from the 15% CF KAPL and Studsvik Alloy 182 in the NiO-stable and Ni-stable regions with respect to the electrochemical potential (ECP) controlled via the DH concentration. In prior discussions with the NRC on the selection of corrosion potential in the NiO and Ni-stable regimes, it was decided that the primary interest was in evaluating relatively small shifts off the Ni/NiO stability line to determine whether SCCI has a strong sensitivity to ECP around the Ni/NiO stability line. This is helpful in understanding variability in SCCI times for tests conducted at the Ni/NiO stability line while also providing some insight into DH effects.

3.4.1 NiO Stable Test

Previous research performed by KAPL indicated that SCCI times of Alloy 600 were substantially longer in the NiO-stable regime while SCCI times in the Ni-stable regime were almost the same as at the Ni/NiO stability line [Etien 2011]. A ΔECP of -7.5 mV relative to the ECP at the Ni/NiO stability line was selected based on the KAPL Alloy 600 results which indicated that SCCI times could be as much as 2x longer even for this small shift in ECP off the Ni/NiO stability line. For this test, which was conducted at 360°C, the corresponding DH content was 20 cc/kg H_2.

Six specimens each from the 15% CF KAPL and Studsvik weldments were tested. Five out of the six KAPL specimens initiated in 60 hours or less, while three of the Studsvik specimens initiated in 35 hours or less. The SCCI behavior of the 12 specimens is shown in Figure 37. After eight specimens initiated in no more than 60 hours, the remaining four specimens did not initiate out to the conclusion of the test at 9969 hours. The results show that the SCCI behavior at -7.5 mV relative to the Ni/NiO stability line is consistent with the results obtained at the Ni/NiO stability line. The extreme difference in SCCI times between the initiated and non-initiated specimens is another clear indicator of the varied response of Alloy 182. Summary information on this test is provided in Table 8.

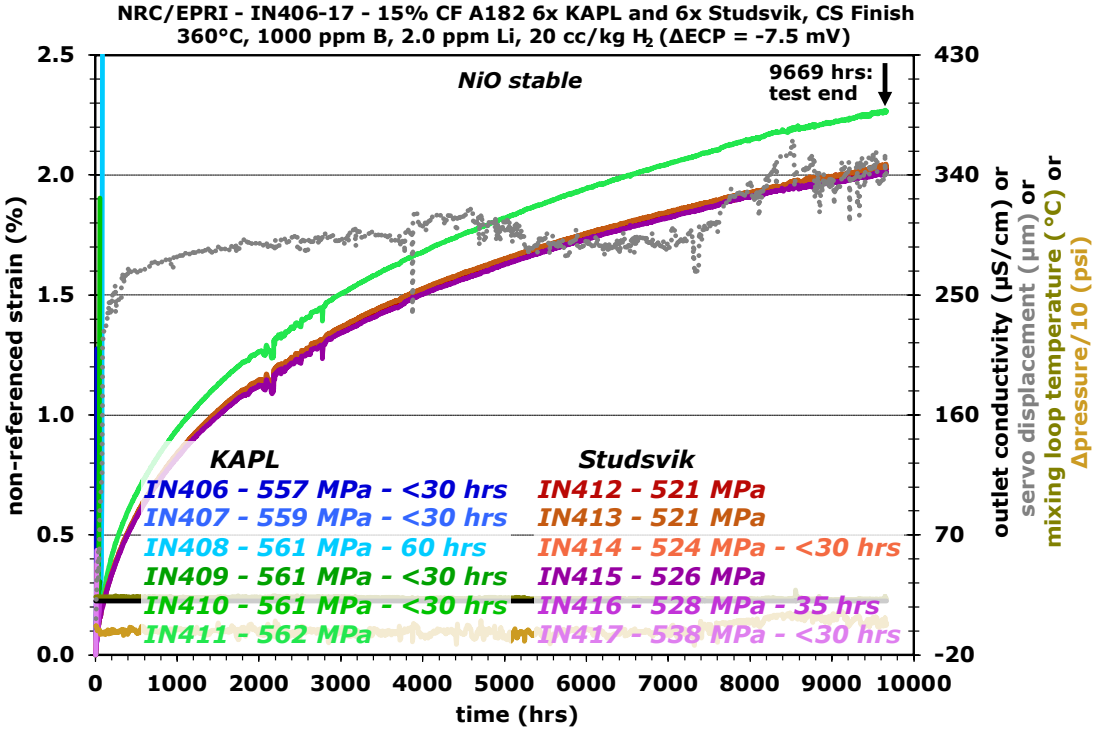

Figure 38. SCCI behavior of 6x each of KAPL and Studsvik 15% CF Alloy 182 tested at 360°C in the NiO-stable regime (ΔECP = -7.5 mV).

Table 8. Summary of six specimens each of two 15% CF Alloy 182 welds tested at their YS at 360°C in the NiO-stable regime with DH set to 20 cc/kg H2 (ΔECP = -7.5 mV). The combined mean, S.D., and median times are 3346, 4683, and 33 hours, respectively.

KAPL	YS (MPa)	t_{init} (h)	Studsvik	YS (MPa)	t_{init} (h)
IN406	557	**<30**	IN412	521	>9669
IN407	557	**<30**	IN413	521	>9669
IN408	561	**60**	IN414	524	**<30**
IN409	561	**<30**	IN415	526	>9669
IN410	561	**<30**	IN416	528	**35**
IN411	562	>9669†	IN417	538	**<30**
Avg., S.D. Sample*		***1692, 3702***	***Avg., S.D. Sample***		***5000, 4969***
Median		***30***	***Median***		***5002***

† The ">" indicates not yet initiated.

** Statistical values are based on exposure time of initiated and non-initiated specimens.

3.4.2 Ni-Metal Stable Test

This was a test on five specimens from the 15% CF Studsvik and six specimens from the 15% CF KAPL Alloy 182 in the Ni-metal stable region. The testing was performed at a ΔECP of +7.5 mV relative to the Ni/NiO stability line at 360°C and at a DH concentration of 35 cc/kg. Alloy 600 SCCI results obtained by KAPL indicated that SCCI times for tests across the entire Ni-metal stability regime would be essentially identical to SCCI times at the Ni/NiO stability line.

The SCCI behavior of the 11 specimens up to the final test time of 88 hours is shown in Figure 38. All five Studsvik and three KAPL specimens initiated in <30 hours. One KAPL specimen initiated at 64 hours and another at 86 hours. These two initiations took place upon restart. The large number of initiation times below 100 hours suggests that 15% CF Alloy 182 is more susceptible to SCCI in the Ni-metal stable regime than at ΔECP near and lower than the Ni/NiO stability line, although more data would be needed, perhaps over a broader range of ΔECP in the Ni-stable region, to effectively assess this. Test results are summarized in Table 9.

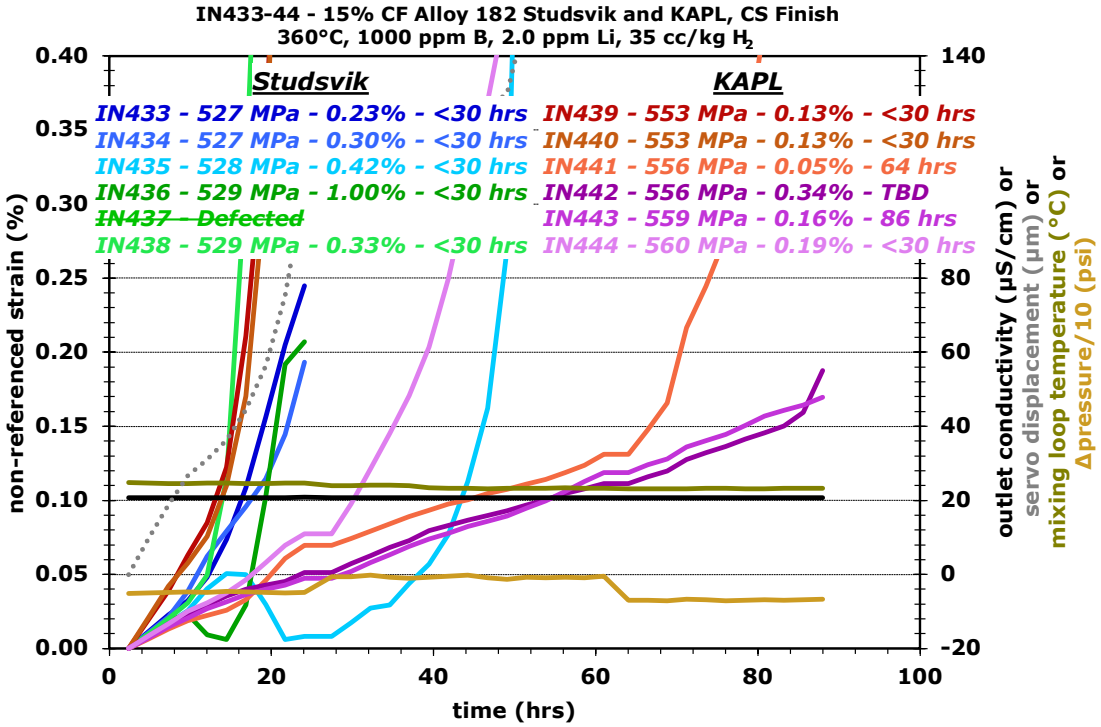

Figure 39. SCCI behavior of five Studsvik and six KAPL 15% CF Alloy 182 specimens tested at 360°C in the Ni-metal stable regime (ΔECP = 7.5 mV).

Table 9. SCCI times for five Studsvik and six KAPL 15% CF Alloy 182 specimens tested at their YS at 360°C in the Ni-metal stable regime with DH set to 35 cc/kg H2 (ΔECP = 7.5 mV). The combined mean, S.D., and median times are 40, 22, and 30 hours, respectively.

Studsvik	YS (MPa)	t_{init} (h)	KAPL	YS (MPa)	t_{init} (h)
IN433	527	**<30**	IN412	553	**<30**
IN434	527	**<30**	IN413	553	**<30**
IN435	528	**<30**	IN414	556	**<30**
IN436	529	**<30**	IN415	556	>88
IN438	529	**<30**	IN416	559	**86**
			IN417	560	**<30**
Avg., S.D. Sample*		***30, 0***	***Avg., S.D. Sample***		***49, 27***
Median		***30***	***Median***		***30***

† The ">" indicates not yet initiated.
** Statistical values are based on exposure time of initiated and non-initiated specimens.

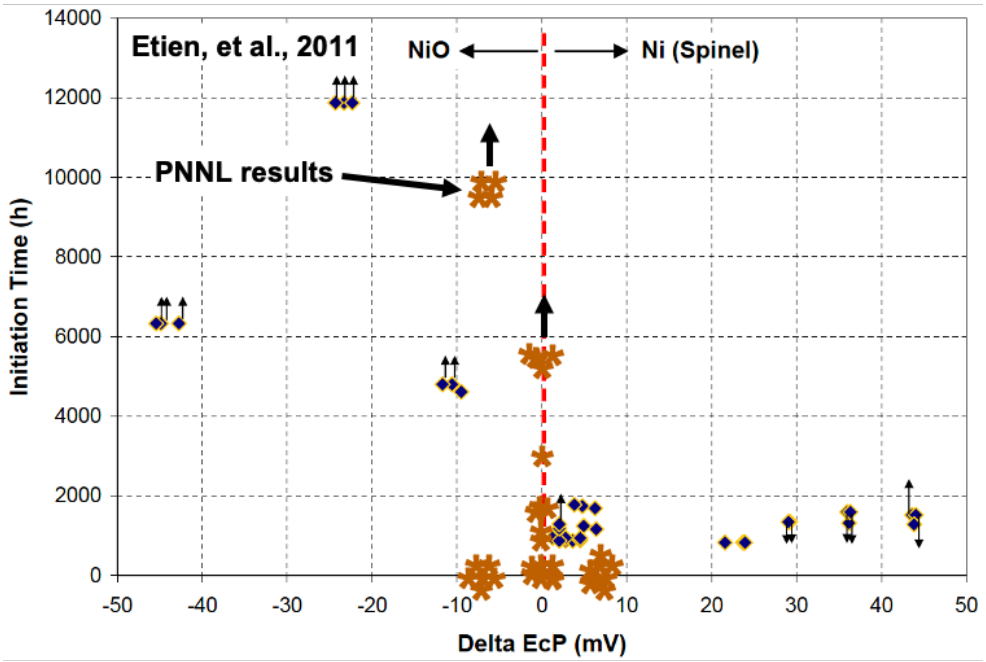

Figure 40. PNNL Alloy 182 DH effects test results compared to KAPL's results on Alloy 600 at 360°C.

3.5 Alloy 182 Tests Conducted at Different Temperatures

The effect of temperature on SCCI time was planned to be evaluated using twelve each of the KAPL and Studsvik Alloy 182 welds in a 15% CF condition. However, there was an insufficient amount of KAPL Alloy 182 weld material, so Phase 2B Alloy 182 material was used instead. These tests are being conducted with the corrosion potential set to correspond to the Ni/NiO stability line to provide a "temperature-only" comparison. These tests are being conducted in the large test systems in groups of 12 specimens with all 12 specimens in a test system instrumented for referenced DCPD strain measurement. This is an ongoing effort with tests planned at 330, 300°C, and one lower temperature that is to be decided, but will likely be either 270 or 280°C.

3.5.1 Alloy 182 Tests Conducted at 330°C

Testing of twelve 15% CF Studsvik Alloy 182 specimens at 330°C with a DH content of 11.5 cc/kg H_2 is complete. The stress versus strain plot during specimen load-up is provided in Figure 40. The obtained plastic strain applied to each specimen during loading ranged from 0.1-0.4% with the exception of the IN366 specimen that went to 1.1% plastic strain during loading. The stresses of 535-551 MPa that were attained during loading to YS are similar to those attained for tests on the 15% CF Studsvik Alloy 182 at 360°C. The non-referenced constant load strain response of the specimens is shown in Figure 41, and a summary of the initiation times is provided in Table 10.

All but one specimen initiated within 982 hours, and 10 out of the 12 specimens initiated within 405 hours. The distribution of SCCI times is qualitatively similar to that observed for this material tested at 360°C in the regard that the majority of the specimens at 360°C and 330°C initiated on the low end of the distribution of initiation times. However, the distribution at 330°C is less skewed because the tail is not a long.

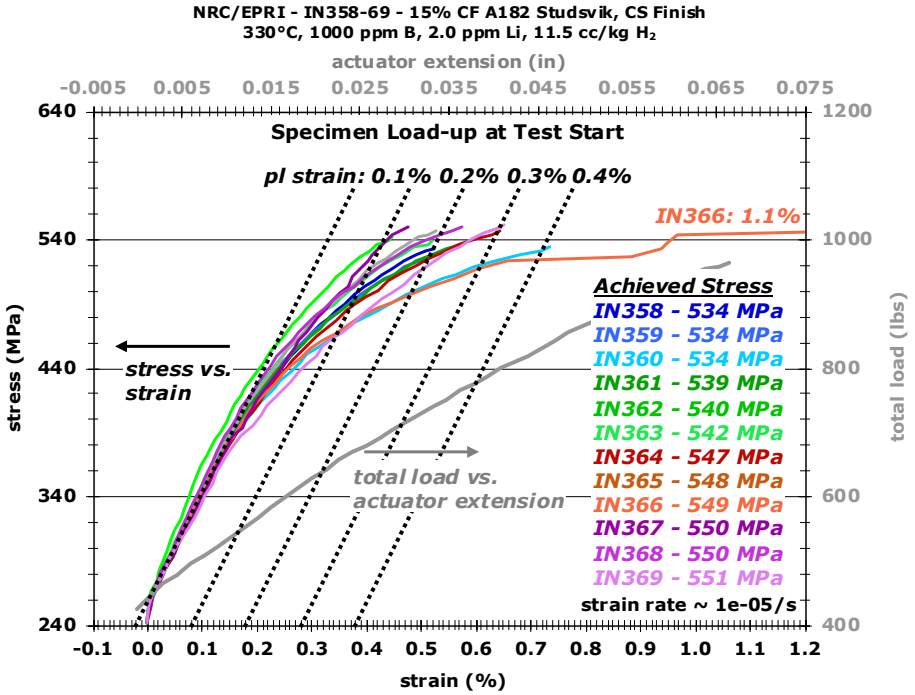

Figure 41. Stress versus strain plot of the 15% CF Studsvik Alloy 182 specimens at the start of SCCI testing at 330°C.

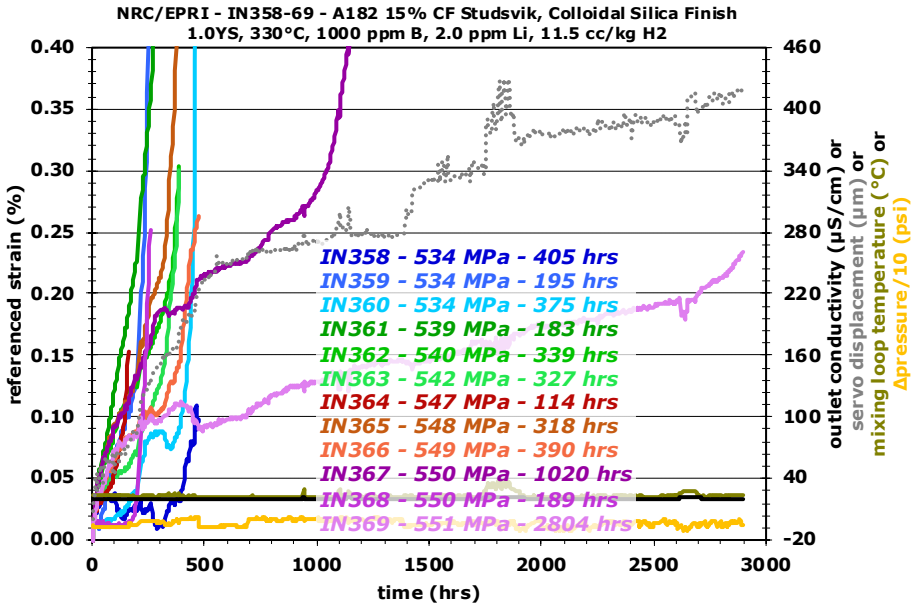

Figure 42. Non-referenced strain response of twelve 15% CF Studsvik Alloy 182 specimens during SCCI testing at 330°C.

Table 10. SCCI times of twelve 15% CF Studsvik Alloy 182 specimens at YS at 330°C with DH set to 11.5 cc/kg H_2.

Studsvik	YS (MPa)	t_{init} (h)
IN358	534	**405**
IN359	534	**195**
IN360	534	**373**
IN361	539	**183**
IN362	540	**339**
IN363	542	**327**
IN364	547	**114**
IN365	548	**318**
IN366	549	**390**
IN367	550	**982**
IN368	550	**189**
IN369	551	**2804**
Avg., S.D. Sample		***552, 743***
Median		***333***

One aspect of SCCI behavior that is of interest is the dependence of SCCI time on applied plastic strain during specimen load-up. This is plotted for the 330°C Studsvik specimens in Figure 42. As was observed for other tests of CF Alloy 182 and Alloy 600, there is significant scatter and no obvious dependence on applied plastic strain during load-up for plastic strains in the range of 0.1-0.4%.

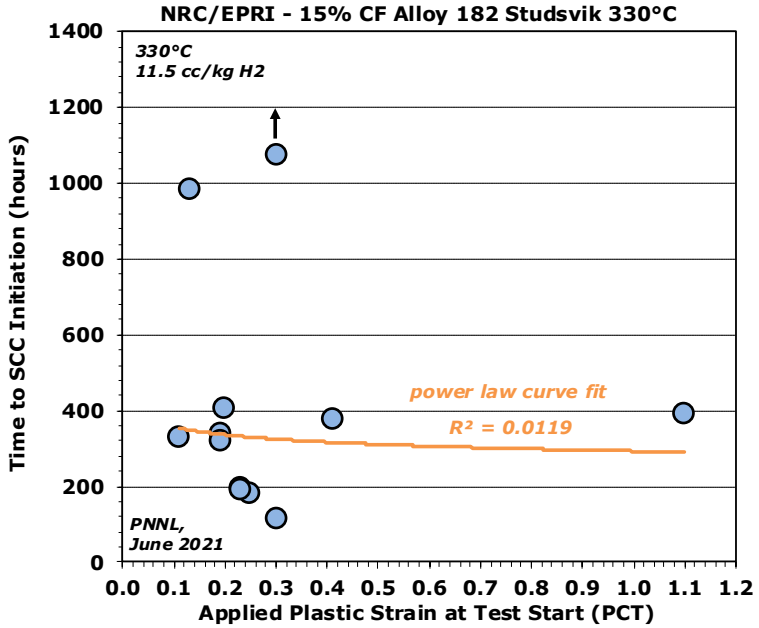

Figure 43. Time to crack initiation plotted against applied plastic strain during load-up for the 330°C Studsvik specimens.

Two sets of tests were conducted on 15% CF Phase 2B Alloy 182 at 330°C because very low SCCI times were observed for the first set of specimens. All specimens initiated almost from the onset of full load. In reviewing the testing conditions for the first set of specimens, it was found that the DH level was 13.2 cc/kg H_2, which is somewhat higher than the intended 11.5 cc/kg H_2 and puts the specimens slightly into the Ni-metal stable regime where lower SCCI times have been observed. The estimated corrosion potential shift off the Ni/NiO stability into the Ni-metal stable regime was 4.6 mV which is approximately 60% of the 7.5 mV offset used to study DH effects in Section 3.4. The DH effects tests reported in Section 3.4 were conducted at 360°C, whereas the DH effect under discussion is for tests at 330°C, so one factor to consider when assessing whether the 4.6 mV shift was sufficient to affect SCCI behavior is whether the strength of the effect of an ECP shift on SCCI is temperature dependent. A study by Morton on DH and ECP effects of Alloy 600 and X-750 indicates that the strength of the ECP effect on SCC behavior is not dependent on test temperature for temperatures in the range under discussion [Morton 2001]. Thus, while the accidental ECP shift of the Ni/NiO stability line was relatively small, it was still enough to be of concern. As a result, it was decided to test a second set of specimens at 11.0 cc/kg H_2 which is right on the Ni/NiO stability line.

The cause of the higher-than-intended DH level was found to be due to gas stratification in the H_2/N_2 mixed gas bottles used to supply hydrogen to the SCC test systems. Although theory indicates that stratification should not occur [Azatyan 2019, Dinh 2020], it nevertheless occurred. The 40% H_2 bottle used for these tests is rarely needed, and as a result, it needs replacing only every 2-3 years. For this series of tests, the bottle was sitting in the hydrogen gas supply cabinet for approximately that length of time. Gas sample measurements revealed that the H_2 composition leaving the bottle was approximately 48%, e.g., the H_2 had somewhat stratified to the top while the N_2 had somewhat stratified to the bottom. Following the recommendation of the mixed gas bottle supplier, the gas bottle was subsequently rolled on the floor for 15 minutes. A follow-on composition measurement gave 40% H_2.

The specimen load-up plot for 15% CF Phase 2B specimens tested at 330°C with DH set to 13.2 cc/kg is provided in Figure 43. All specimens behaved very similarly with the range of applied plastic strain varying between 0.21-0.43%. A tight range of stresses was also obtained. Constant load referenced strain response is presented in Figure 44. Within 30 hours of full load exposure, the strain evolution of each specimen exhibited significant positive curvature indicating that crack initiation had occurred. Post-test examination of the specimens revealed a very high number of SCC cracks on each specimen as shown for example in Figure 45 for the IN511 which exhibited a below mid-range SCCI response.

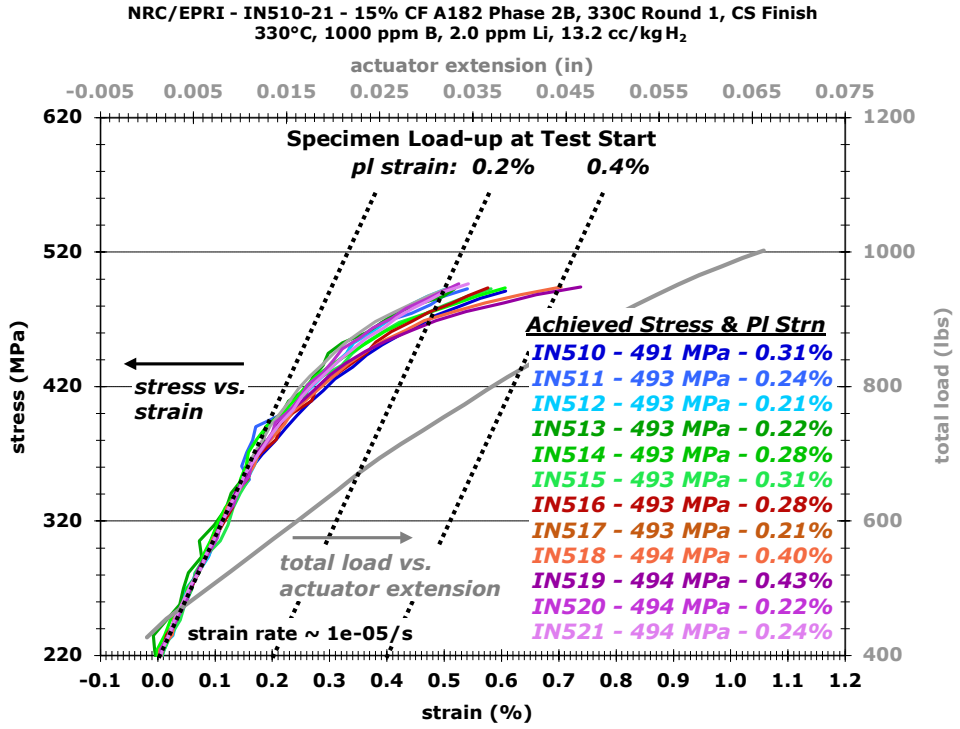

Figure 44. Stress versus strain plot of the first set of 15% CF Phase 2B Alloy 182 specimens at the start of SCCI testing at 330°C. DH was 13.2 cc/kg H_2 for these specimens.

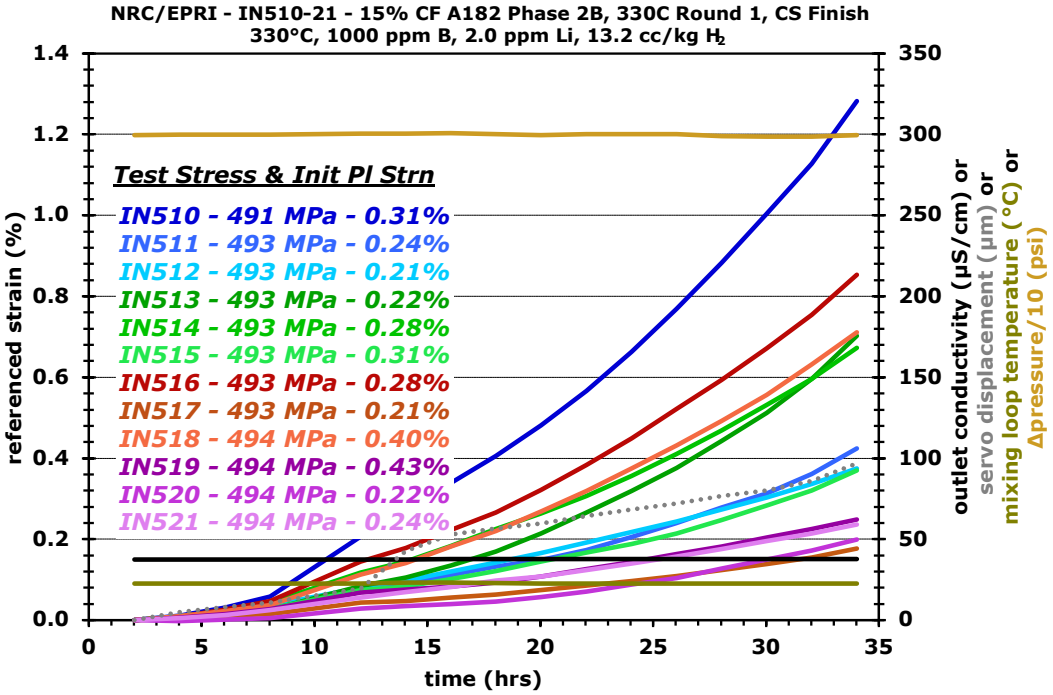

Figure 45. Referenced strain response of the first set of 15% CF Phase 2B Alloy 182 specimens at 330°C. DH for these specimens was 13.2 cc/kg H_2.

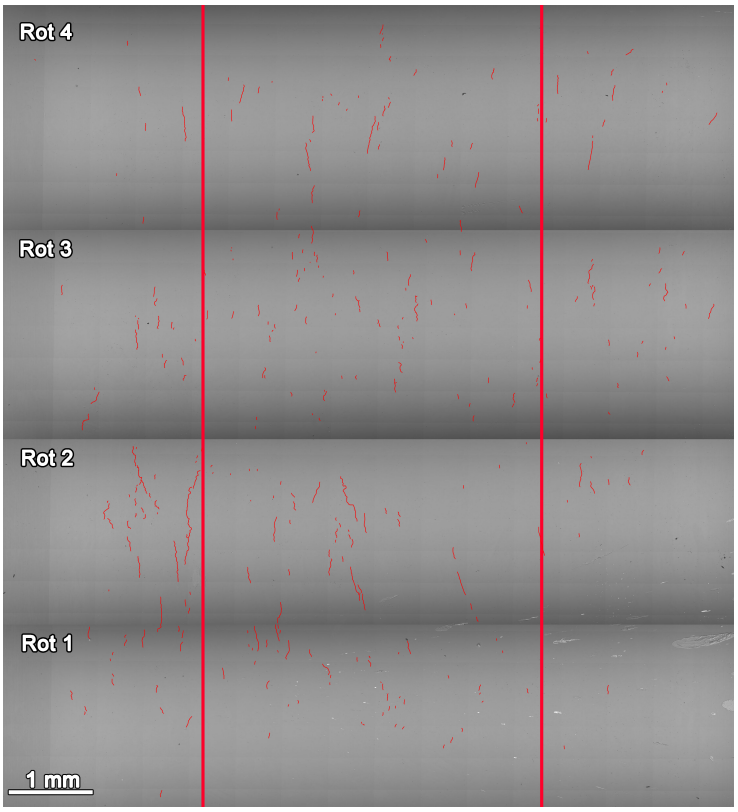

Figure 46. Post-test surface crack identification of IN511 (15% CF Phase 2B Alloy 182).

The stress versus strain load-up plot for the second set of 15% CF Phase 2B Alloy 182 specimens is shown in Figure 46. For this test, a fully mixed H_2/N_2 bottle was used, and the DH level was 11.0 cc/kg. As with the first set of specimens, the loading process went ideally with applied plastic strains ranging from 0.2-0.35% and applied stresses ranging from 494-499 MPa. The obtained stresses and strains are virtually identical to the first batch of specimens that were tested. The constant load referenced strain plot in Figure 47 shows that this second set of specimens behaved almost identically to the first set of specimens. Observed SCCI times were just slightly longer for these specimens. SCCI times for the first and second set of specimens are listed in Table 11.

When considering the SCCI behavior at 330°C, both the Studsvik and the Phase 2B specimens all underwent SCCI, and the observed initiation times were not strongly different. This is in contrast to the tests at 360°C where a small number of specimens either exhibited long initiation times or did not initiate. So, in this way, the Studsvik and Phase 2B welds behaved similarly at 330°C. However, there was still a strong difference in their response with the Phase 2B weld undergoing very rapid SCCI while the Studsvik exhibited somewhat longer SCCI times. The reasons for the difference in behavior are not understood at this time.

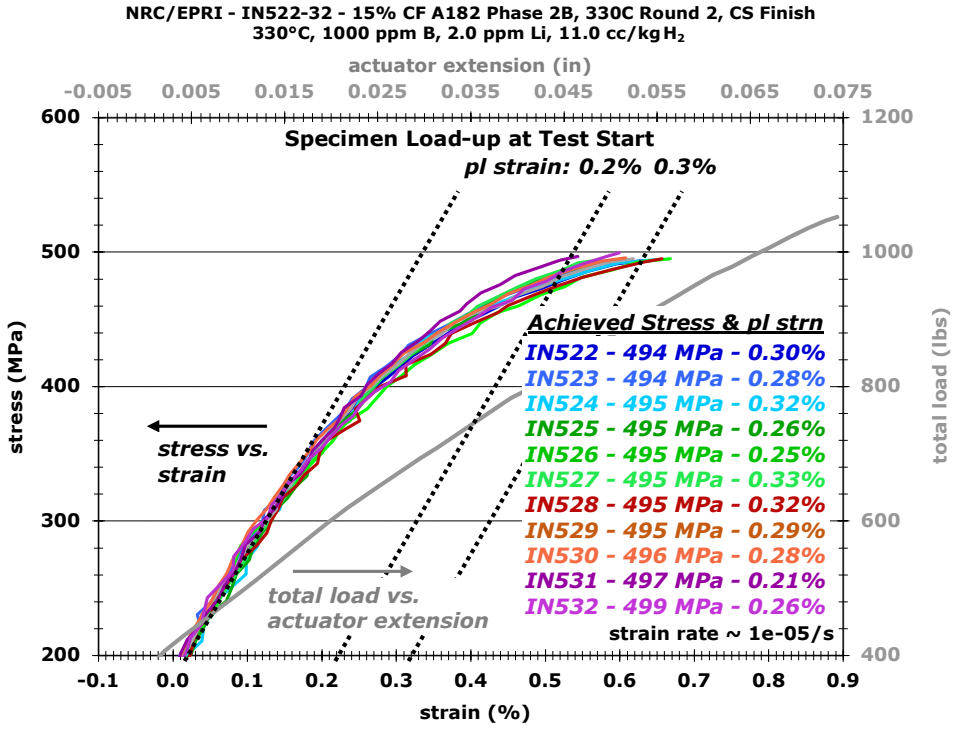

Figure 47. Stress versus strain plot of the second set of 15% CF Phase 2B Alloy 182 specimens at the start of SCCI testing at 330°C. DH was 11.0 cc/kg H_2.

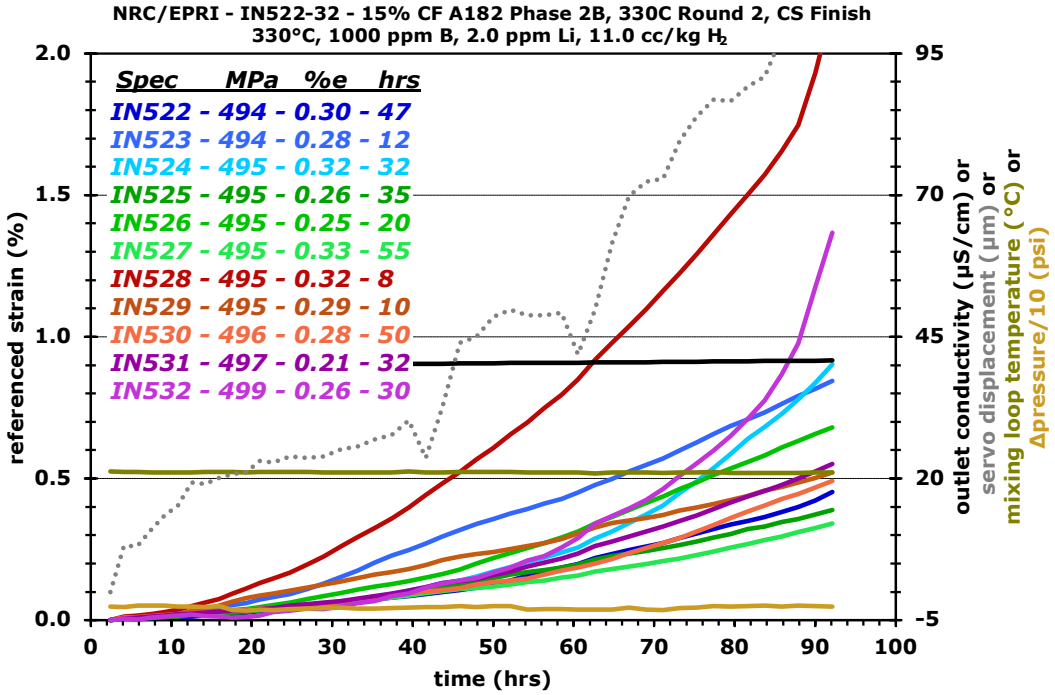

Figure 48. Referenced strain response of the second set of 15% CF Phase 2B Alloy 182 specimens at 330°C. DH for these specimens was 11.0 cc/kg H_2.

Table 11. SCCI times for 15% CF Phase 2B Alloy 182 specimens tested at YS at 330°C. IN510-21 had a DH content of 13.2 cc/kg which is slightly Ni-metal stable while IN522-32 had a DH content of 11.0 cc/kg which is very slightly NiO-stable.

Phase 2B	YS (MPa)	t_{init} (h)	Phase 2B	YS (MPa)	t_{init} (h)
IN510	491	**≤30**	IN522	494	**30**
IN511	493	**≤30**	IN523	494	**≤30**
IN512	493	**≤30**	IN524	495	**30**
IN513	493	**≤30**	IN525	495	**30**
IN514	493	**≤30**	IN526	495	**≤30**
IN515	493	**≤30**	IN527	495	**30**
IN516	493	**≤30**	IN528	495	**≤30**
IN517	493	**≤30**	IN529	495	**≤30**
IN518	494	**≤30**	IN530	496	**30**
IN519	494	**≤30**	IN531	497	**30**
IN520	494	**≤30**	IN532	499	**30**
IN521	494	**≤30**			
Avg., S.D. Sample		***≤30, N/A***	***Avg., S.D. Sample***		***≤30, N/A***
Median		***≤30***	***Median***		***≤30***

** Statistical values are based on exposure time of initiated and non-initiated specimens.

3.5.2 Alloy 182 Tests Conducted at 300°C

The test on the Studsvik material at 300°C and 5.2 cc/kg H_2 (corresponding to the Ni/NiO stability line) is complete. The initiation times are listed in Table 11. Although the shortest SCCI times are longer than at 330 and 360°C, the 300°C initiation times have a lower average and median time than the Studsvik test conducted at 330°C. The reason for this is that the tail of the distribution is even shorter at 300°C than at 330 and 360°C. There is almost no skew in the distribution. As will be discussed in Section 3.5.3, this complicates determination of an activation energy.

Specimens are being prepared for a 300°C test of twelve 15% CF Phase 2B Alloy 182 specimens. These results will be provided in a future report.

Table 12. SCCI times of twelve 15% CF Studsvik Alloy 182 specimens tested at their YS at 300°C and 5.2 cc/kg H_2.

Studsvik	YS (MPa)	t_{init} (h)
IN421	538	**225**
IN422	540	**395**
IN423	540	**327**
IN424	540	**360**
IN425	540	**440**
IN426	541	**385**
IN427	541	**255**
IN428	541	**246**
IN429	541	**300**
IN430	543	**231**
IN432	543	**303**
IN432	543	**240**
Avg., S.D. Sample		***309, 73***
Median		***302***

SCCI testing at 300°C was also conducted on a set of three 15% CF EWI Alloy 182 specimens. This material exhibited ≤30 hour SCCI times at 360°C, so there was interest in evaluating whether it would exhibit shorter or longer SCCI times when tested at 300°C. As can be seen in the summary of the test results in Table 13, low SCCI times were observed for these specimens.

Table 13. SCC initiation times for three 15% CF Alloy 182 EWI specimens tested at 300°C with DH set to 5.2 cc/kg H_2.

EWI	YS (MPa)	t_{init} (h)
IN418	531	**30**
IN419	532	**40**
IN420	532	**40**
Avg., S.D. Sample		***37, 6***
Median		***40***

3.5.3 15% CF Studsvik Alloy 182 Temperature Dependence

If the average initiation time is used, an activation energy of -63 kJ/mol (**a negative value**) is obtained because the average initiation time of the Studsvik tests at 360°C is longer than at 330 and 300°C. If the median initiation time is used, the activation energy is positive and has a value of 64 kJ/mol which is approximately half of the reported activation energy for SCCI for Alloy 600 [Etien 2011, Zhai 2020] and less than half that of Alloy 182 [Troyer 2015]. It is half the SCCGR activation energy of Alloy 182 and Alloy 600 [White 2002, White 2004]. The large difference in activation energy associated with the two different statistical parameters is because the distribution of SCCI times is different at each temperature. Histograms for the Studsvik SCCI data are presented in Figures 48, 49, and 50 for the 360, 330, and 300°C data,

respectively. The bins are 100 hours wide, and the center of the bins is used for plotting. In these plots, it can be seen that as the test temperature is increased from 300 to 360°C, the distribution of initiation times becomes progressively more right-skewed which causes the average and mean value to diverge from each other at higher temperatures. It is the divergence that causes the different activation energy for the two parameters.

The difference in activation energy for the two statistical parameters bares consideration in which parameter is most appropriate for activation energy measurement. The goal of the effort is to characterize typical behavior. In highly skewed populations, the average value is not representative of typical behavior. This is evident in the highly right-skewed histogram for the 360°C tests where the average initiation time is 1105 hours, but almost half of the initiations occurred below 100 hours. The median initiation time of 83 hours at 360°C is much more representative of the typical behavior, and thus it is more appropriate to use.

Another statistical parameter that can be used is the mode which is the most probable value in a distribution. This value represents the most frequently observed initiation time. The mode can be determined by several methods depending on the data type. For a set of discrete data, the mode is the most frequently occurring value in the data set. For continuous data sets such as a set of SCCI times, the mode can be determined via computation methods if there is a sufficient amount of data [Grenander 1965, Bickel 2002, Bickel 2006]. Another approach to determining the most probable value in a continuous data set is to use a binning method. In this approach, the data are binned into groups, and then the mode can be determined from the following formula:

$$M = \left(\frac{b_{m-1} f_{m-1} + b_m f_m + b_{m+1} f_{m+1}}{f_{m-1} + f_m + f_{m+1}} \right) \qquad \text{Equation 4}$$

where:

f_m is the frequency (number of members) of the modal class bin

f_{m-1} is the frequency of the bin preceding the modal class bin

f_{m+1} is the frequency of the bin succeeding the modal class bin

b_m is the value of the middle of the modal class bin

b_{m-1} and b_{m+1} are for the preceding and succeeding bins

This approach relies on manual identification of the modal class bin. The mode value is refined within the width of that bin based on bin width and the number of members of the preceding and succeeding bins. This is a first order, nearest neighbor refinement of the mode value with the modal class bin.

For the Studsvik Alloy 182 at 360°C, the most probable initiation time is within the 100-hour bin, and the manual mode estimation method gives a value of 50 hours. At 330°C, the two most populated bins are the 150 hour and 350-hour bins. There are no initiations inside the 250-hour bin. It could be argued that this is a bi-modal dataset, but in the context of the SCCI data that has been obtained for this project, this is an unlikely way to frame this dataset. Instead, it is more reasonable to assume a single mode with the mode initiation time within the 250-hour bin. The manual method gives a mode of 261 hours. For the test at 300°C, the mean, median, and mode are all virtually identical and have a value of approximately 300 hours. A summary of the mean, median, and mode (i.e., most probable values) at each test temperature is listed in Table 14.

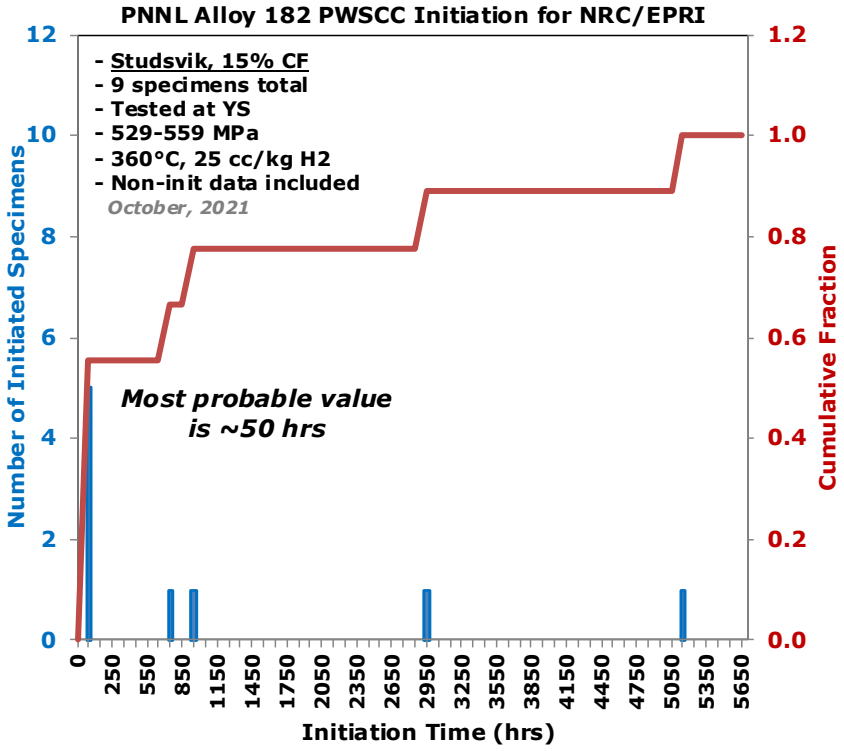

Figure 49. Distribution of 15% CF Studsvik Alloy 182 at 360°C.

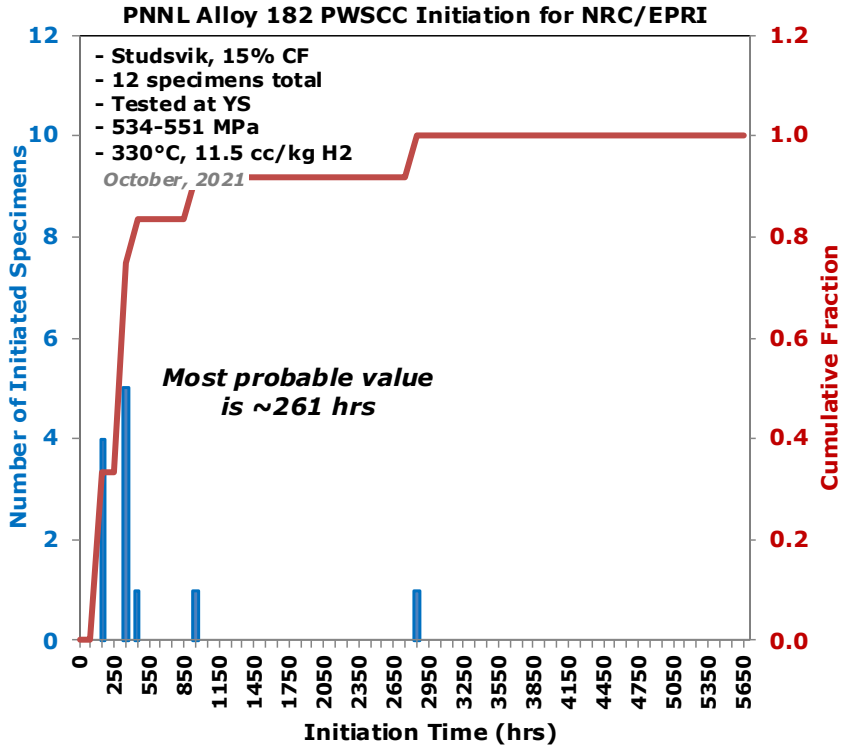

Figure 50. Distribution of 15% CF Studsvik Alloy 182 SCCI times at 330°C.

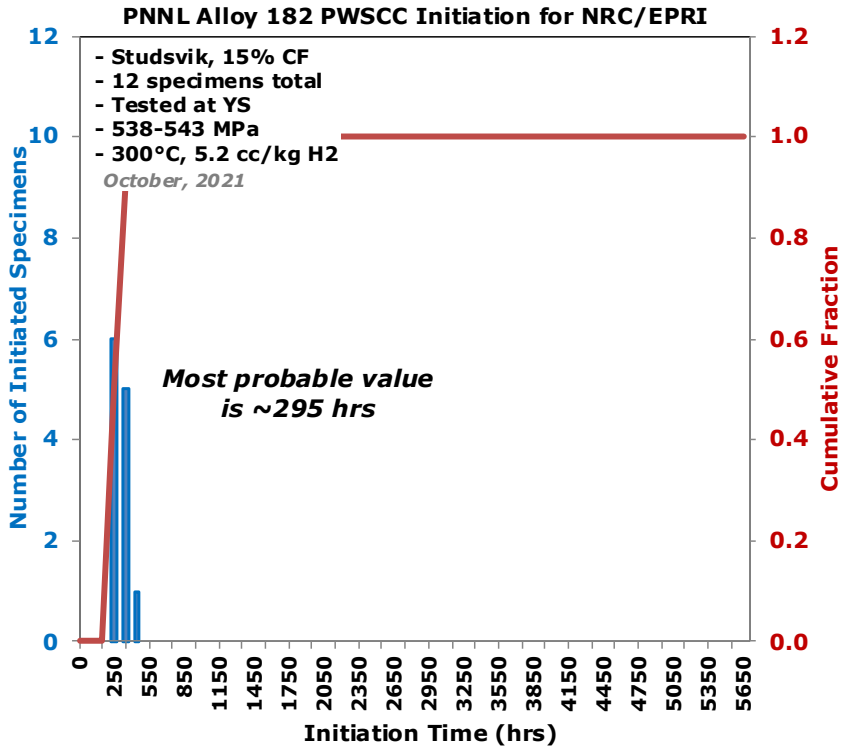

Figure 51. Distribution of 15% CF Studsvik Alloy 182 SCCI times at 300°C.

Table 14. Summary of statistical values obtained from the Studsvik Alloy 182 tests conducted at 360, 330, and 300°C.

Test Temperature (C)	Mean SCCI Time (h)	Median SCCI Time (h)	Most Probable SCCI Time (h)
360	1105	83	50
330	552	333	261
300	309	302	295

Activation energy evaluations for these three different approaches to defining a representative response are illustrated in Figure 51. The mode-based activation energy is 89 kJ/mole which is slightly higher than the median-based activation energy. As previously noted, the activation energy for SCCI of Alloy 600 in the same temperature range is approximately 140 kJ/mole and the estimate of the activation energy for Alloy 182 is 185 kJ/mol [Troyer 2015].

Figure 52. Activation energy for SCCI time of 15% CF Studsvik Alloy 182 using three different assessments of representative SCCI behavior of the material.

4.0 Alloy 600 Testing Status

This task is being conducted partly to determine an FOI in initiation time for Alloy 690 over Alloy 600. Alloy 600 SCCI time measurements also provide a point of comparison for Alloy 182 SCCI initiation behavior. The four heats of Alloy 600 evaluated for this project are described in Table 15, and their composition is provided in Table 16. Optical images of the microstructure at the grain size level were obtained for NX6106XK-11, 522068, and WNP5 and are shown in Figures 52 through 54. Each of these three materials has significant differences in grain appearance. NX6106XK-11 has a wide range of grain sizes and grain shapes. 522058 has a more uniform grain size, but the grains are significantly larger than the other two materials. WNP5 grains are similar in average size to NX6106XK-11, but the size is more uniform. All three materials contain both matrix and grain boundary precipitates. All tests were conducted on 15% CF Alloy 600.

Table 15. The heats of Alloy 600 evaluated for this project.

Source	Heat #	Product Form	Heat Treat Condition
Special Metals	NX6106XK-11	2.0” thick plate	Mill annealed - 927C/3.5h/WQ
G.O. Carlson	33375-2B	2.0” thick plate	Mill annealed - details not provided
ATI	522068	3.0” thick plate	Mill annealed - details not provided
Washington Nuclear Power Reactor #5	Unknown, named “WNP5”	CRDM* tubing	Unknown

*CRDM: Control rod drive mechanism

Table 16. Composition of the four heats of Alloy 600 evaluated for this project.

Heat #	Composition Source	C	Cr	Ni	Si	Mn	Cu	S	P	Fe
NX6106XK-11	CMTR*	0.06	16.4	74.0	0.22	0.23	0.01	0.001	0.004	8.5
33375-2B	CMTR	0.064	14.7	76.7	0.34	0.36	0.04	0.001	NP**	7.2
522068	CMTR	0.052	16.1	73.9	0.14	0.21	0.08	<0.001	0.008	9.3
WNP5	Laboratory	0.03	16.5	76.3	0.35	0.28	0.01	<0.001	<0.005	6.0
Specification	ASTM	0.05-0.15	14.0-17.0	72.0 min	0.5 max	1.0 max	0.50 max	0.015 max	0.015 max	6.0-10.0

*CMTR: Certified material test report
**NP: Not provided.

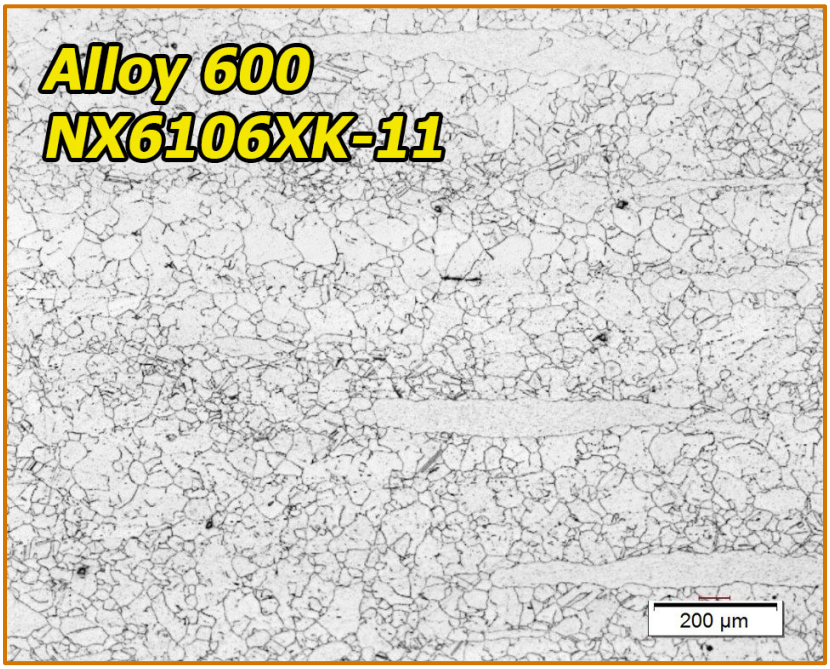

Figure 53. Optical image of Alloy 600 NX6106XK-11 heat microstructure in mid-thickness of the CRDM tubing wall where specimens are extracted.

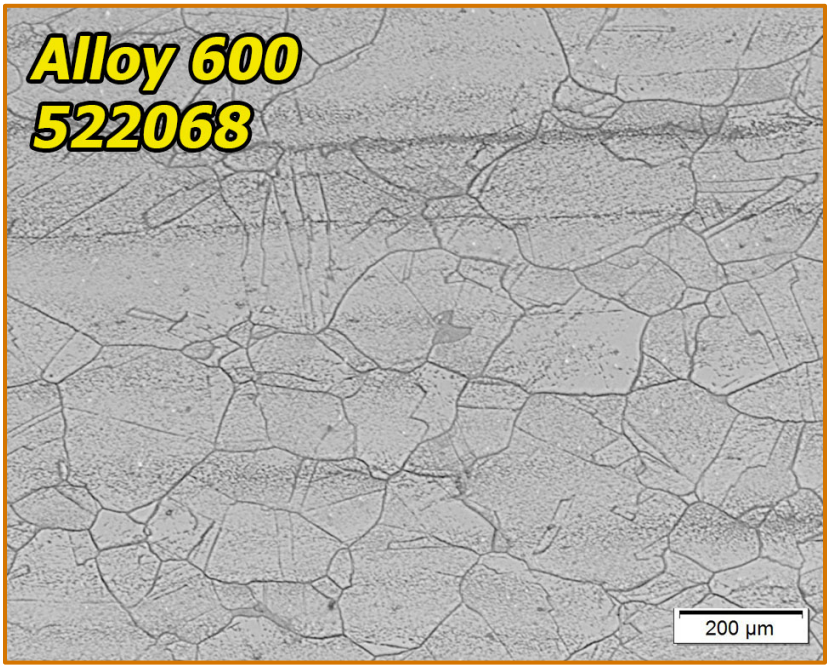

Figure 54. Optical image of Alloy 600 522068 heat microstructure in mid-thickness of the CRDM tubing wall where specimens are extracted.

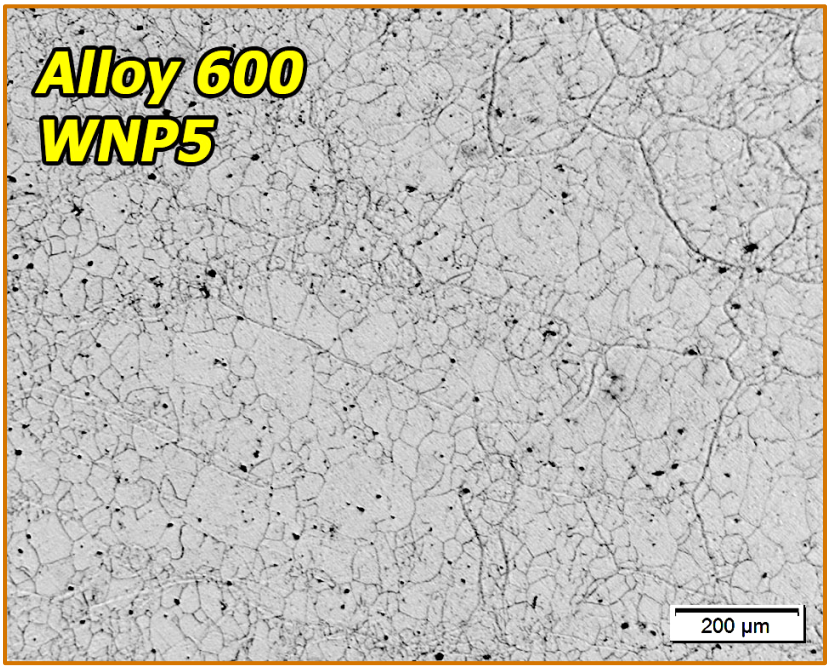

Figure 55. Optical image of Alloy 600 WNP5 CRDM heat microstructure in mid-thickness of the CRDM tubing wall where specimens are extracted.

4.1 Alloy 600 Tests Conducted at Yield Stress Loading

Tests were conducted on nine specimens of each of the four heats. Details of some of the tests on the NX6106XK-11 and 33375-2B heats are available in the 2017 report [Toloczko 2017]. The detailed SCCI behavior of heats 522068 and WNP5 are provided in the current report.

4.1.1 SCCI Tests of Heat 522068 at 1.0YS

Testing of these specimens was broken into a group of three specimens tested early in the program and a group of six tested a few years later. Specimen loading runs for the two groups are provided in Figures 55 and 56. The set of three specimens was loaded to approximately 0.2% plastic strain, while the set of six specimens exhibited a wider range of plastic strains during loading that ranged from 0.20-0.47%. The final stresses for the set of three specimens were all 450 MPa while the final stresses for the group of six specimens ranged from 472 to 475 MPa.

Strain versus time plots at constant load for the two sets of specimens are provided in Figures 57 and 58. Heat 522068 consistently exhibited a very gradual initiation transition which created some challenge in defining the time of initiation which is typically the point of inflection to a rapidly increasing slope. For these specimens, a transition to a more rapid slope increase was used. Arrows signify the point of initiation. The very gradual transition suggests that this material exhibits lower SCC growth rates.

SCCI times for the group of three specimens ranged from 840-890 hours while the initiation times for the group of six specimens was lower and ranged from 480-715 hours. The lower SCCI times for the group of six specimens could be due to the slightly higher stress on those specimens, or it could just be variability in material response. However, it cannot be attributed to differences in applied plastic strain among the two groups of specimens because the applied

plastic strain for the group of six was equal or greater than the plastic strain for the group of three specimens but had significantly longer SCCI times.

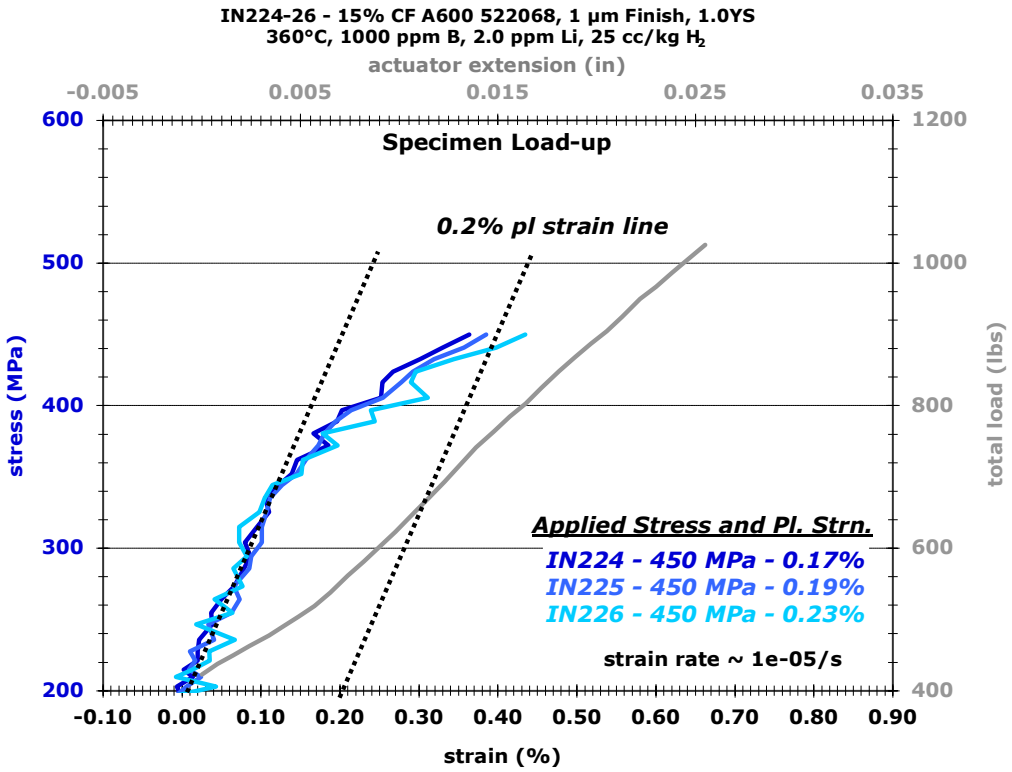

Figure 56. IN224-26 15% CF Alloy 600 heat 522068 load-up at test start.

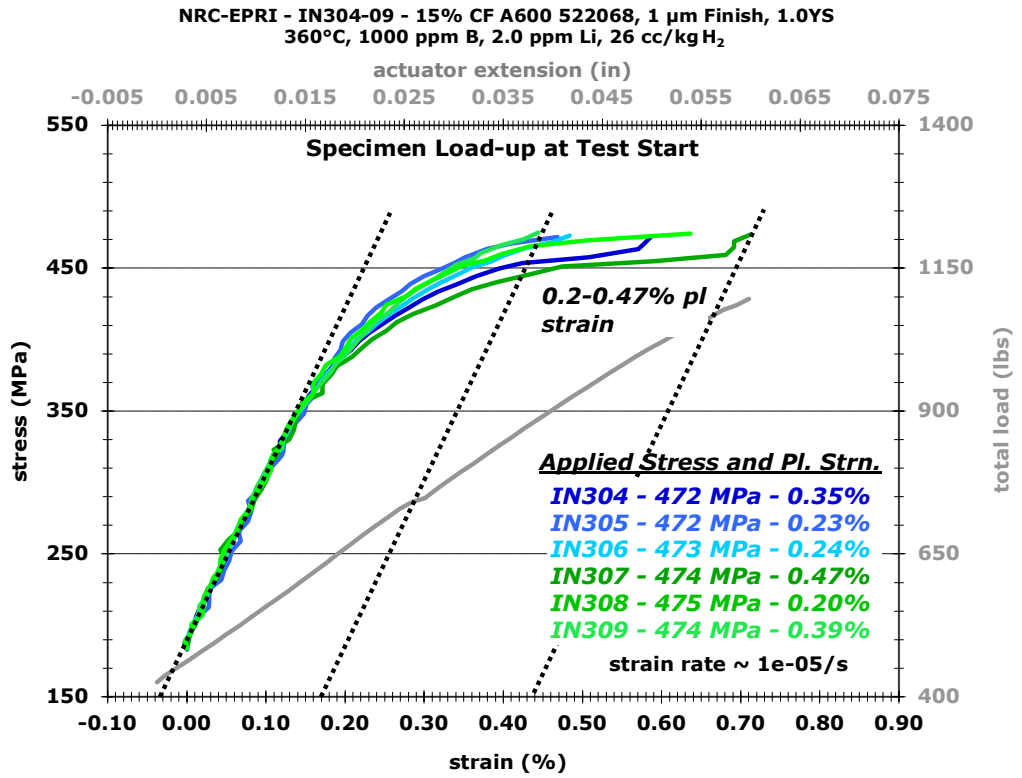

Figure 57. IN304-09 15% CF Alloy 600 heat 522068 load-up at test start.

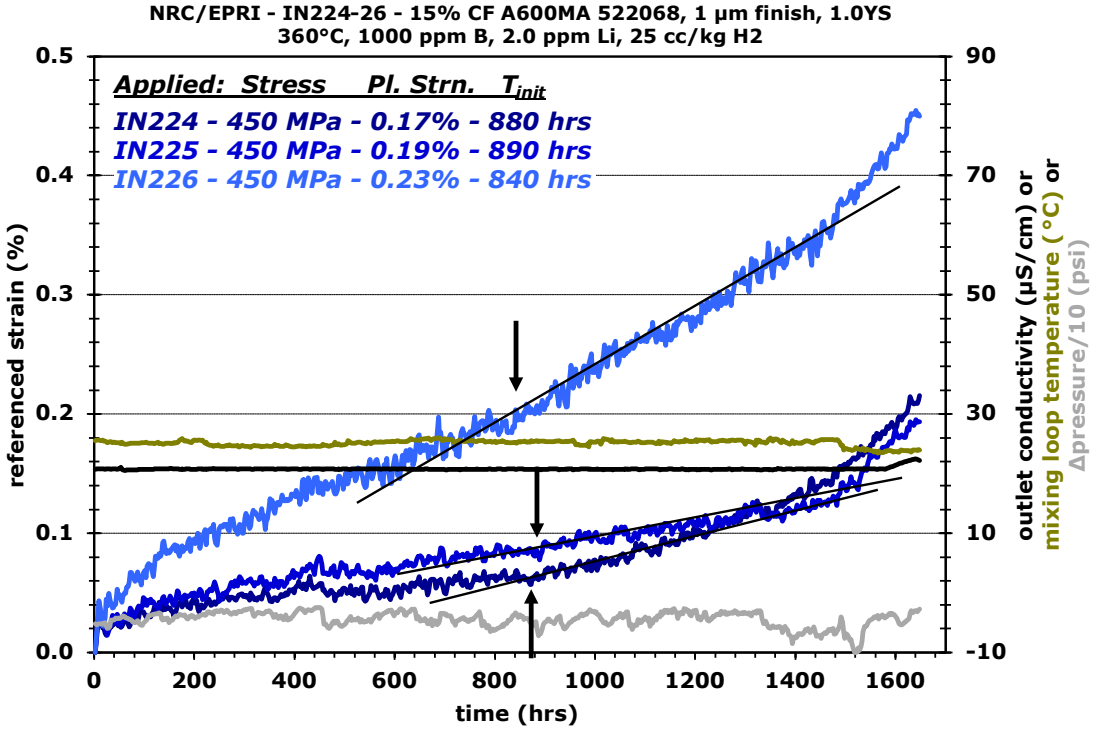

Figure 58. IN224-26 15% CF Alloy 600 heat 522068 constant load SCCI response.

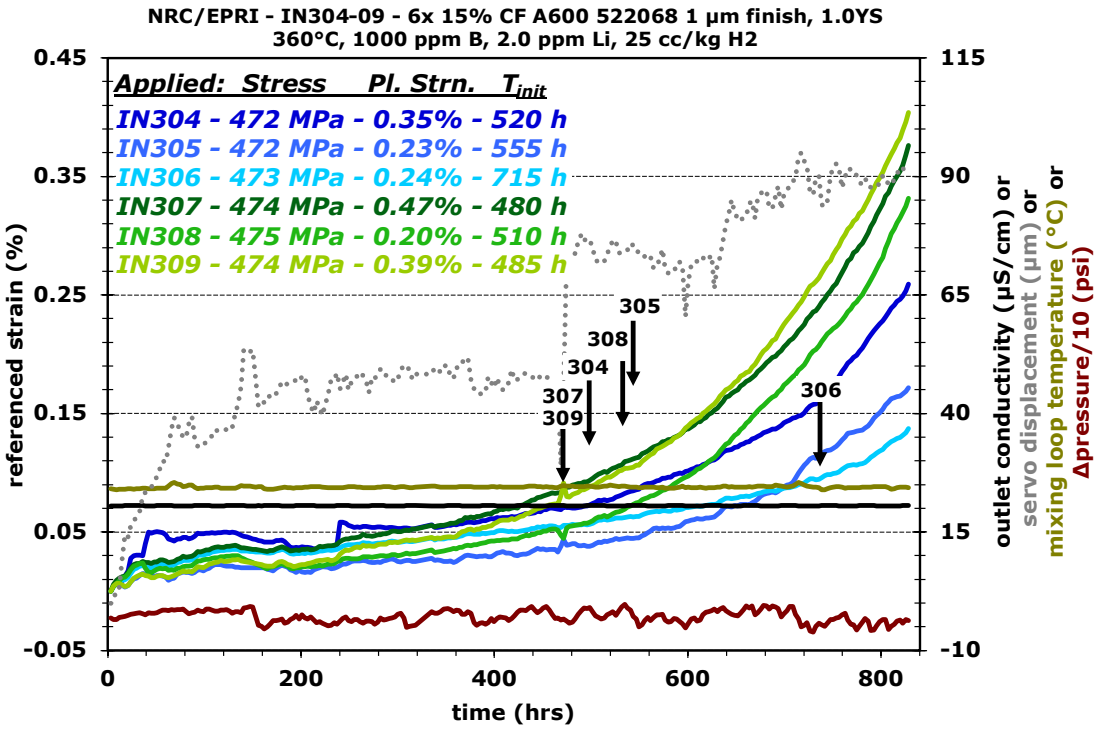

Figure 59. IN304-09 15% CF Alloy 600 heat 522068 constant load SCCI test at 1.0YS.

4.1.2 SCCI Tests of Heat WNP5 at 1.0YS

Testing of the WNP5 specimens was broken into a group of three and a group of six that were run almost sequentially. Specimen loading runs for the two groups are provided in Figures 59 and 60. Applied strains and stresses were nearly identical for the two groups of specimens. The group of three were taken to 0.21-0.22% plastic strain while the group of six were taken to 0.2-0.3% plastic strain. Applied stresses among the two groups of specimens were also very similar with the group of six having stresses that were only 3% higher than the group of three.

Strain versus time plots at constant load are shown in Figures 61 and 62. This heat of Alloy 600 tends to exhibit a sharp initiation transition when in a 15% CF condition as can be seen in the plots. Initiation times among the two sets of specimens were very similar. Only one specimen out of the nine exhibited a significantly different (lower) SCCI time than the other specimens.

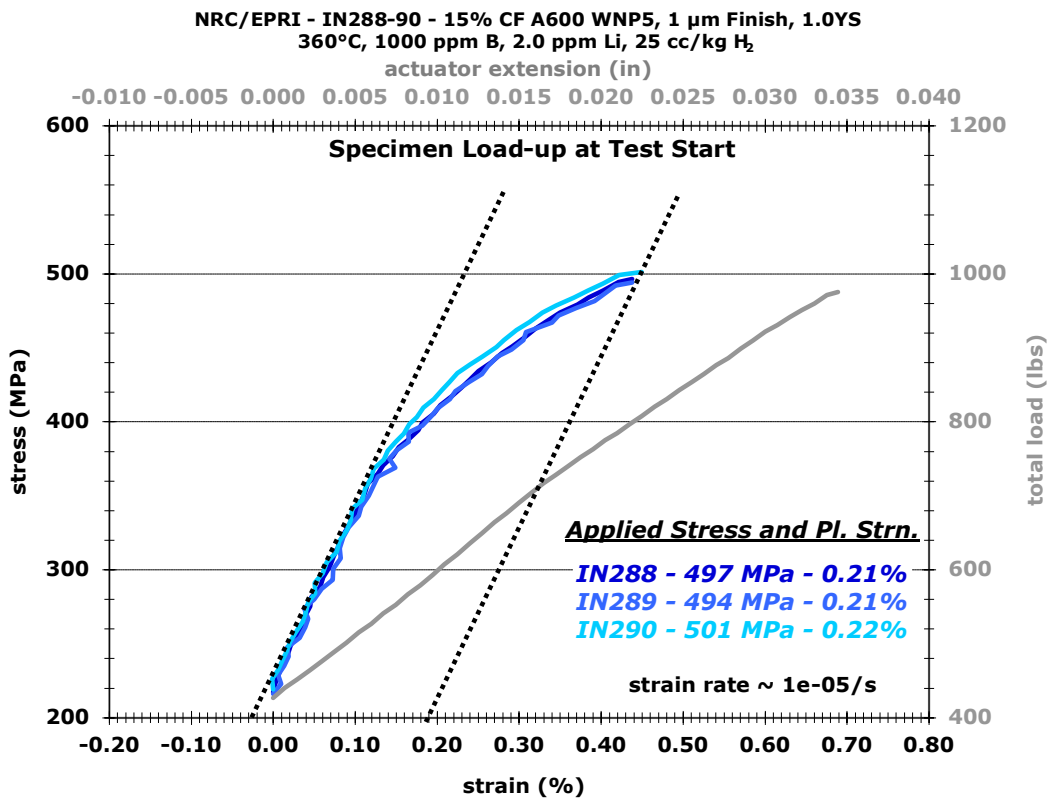

Figure 60. IN288-90 15% CF Alloy 600 heat WNP5 load-up at test start.

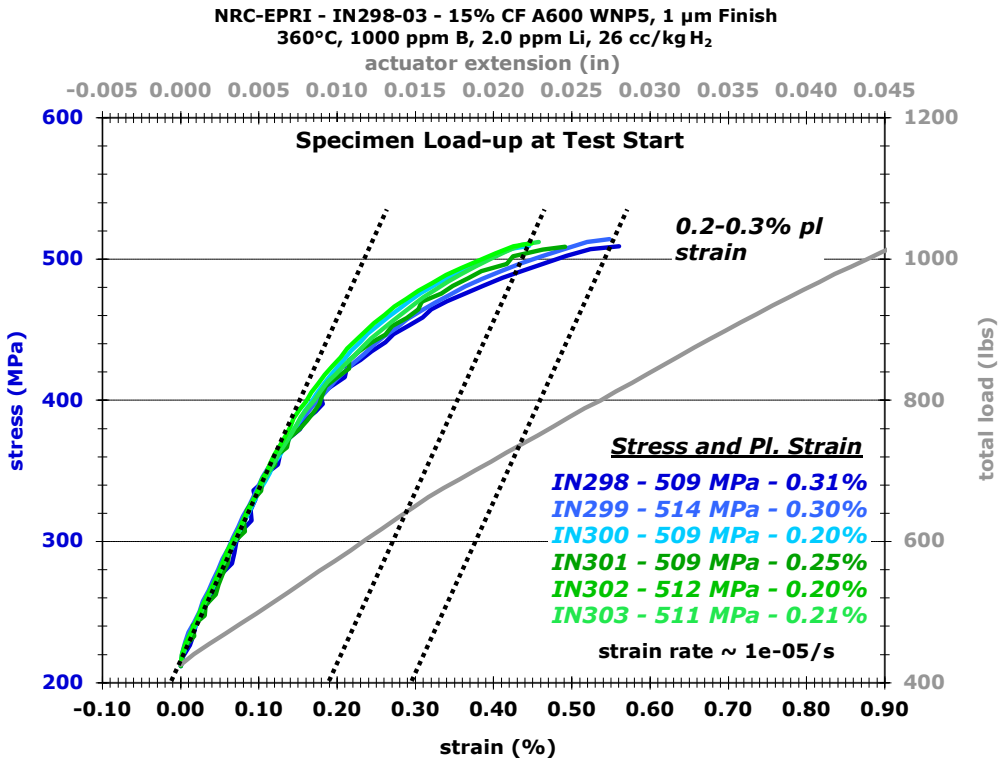

Figure 61. IN298-303 15% CF Alloy 600 heat WNP5 load-up at test start.

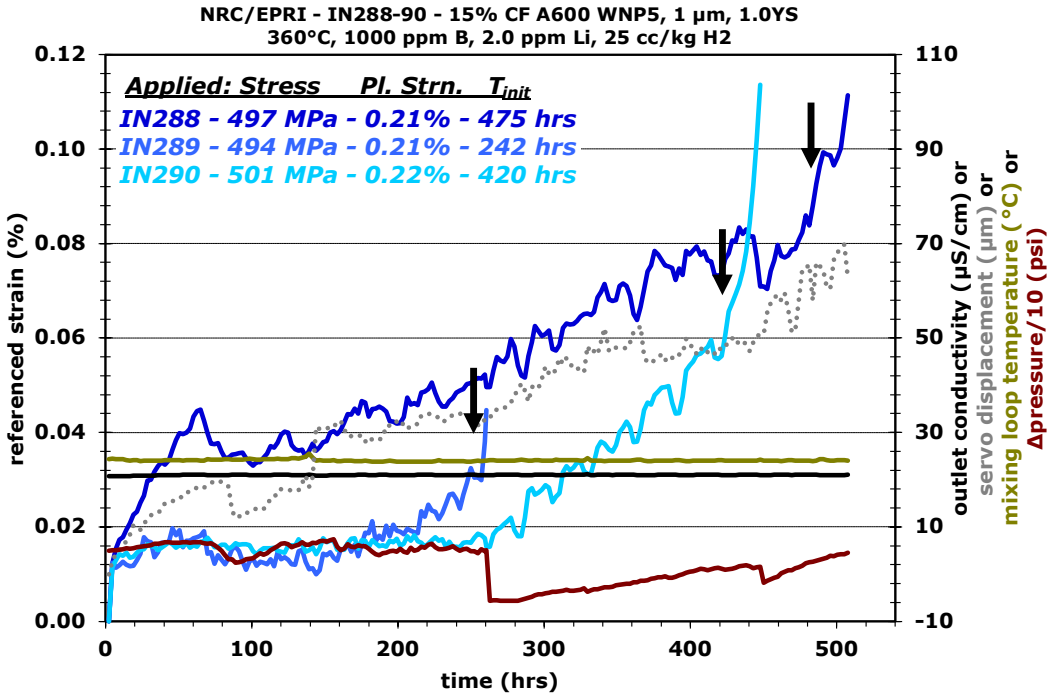

Figure 62. IN288-90 15% CF Alloy 600 heat WNP5 constant load SCCI response.

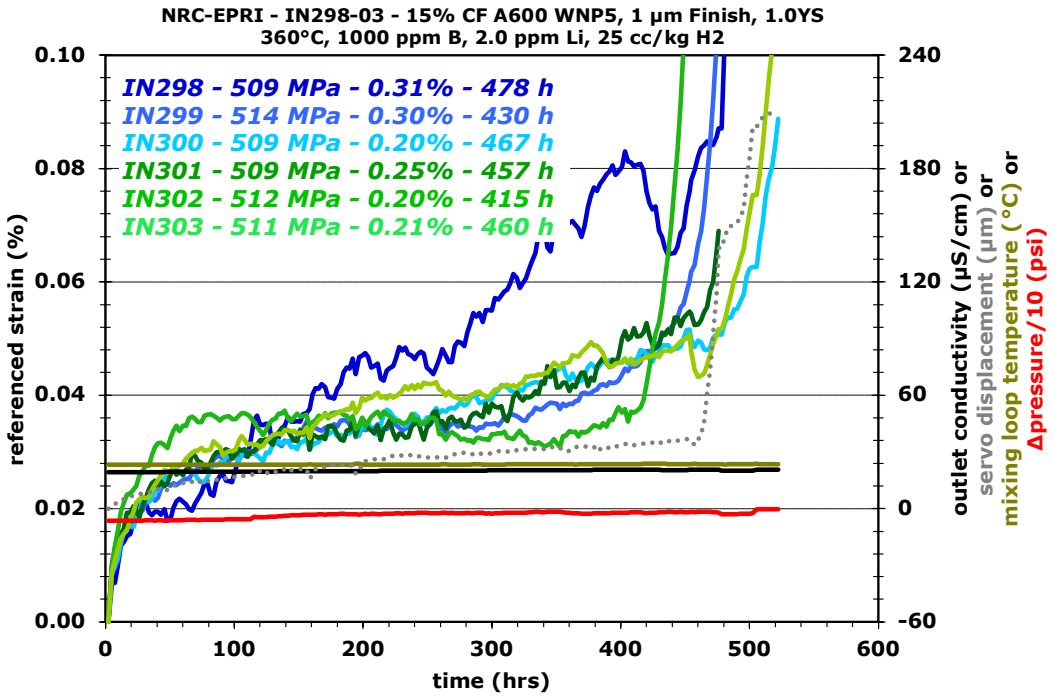

Figure 63. IN298-303 15% CF Alloy 600 heat WNP5 constant load SCCI response.

4.1.3 Discussion of 15% CF Alloy 600 SCCI Results at 1.0YS

The initiation times are summarized in Table 17. Six of the NX6106XK-11 specimens were tested under less-than-ideal conditions, likely resulting in longer initiation times. These six specimens along with six other specimens were tested together as IN154-IN165 in a large autoclave in a 3-string configuration (four specimens on each string). IN163 (1062 hour initiation time) was accidentally allowed to fail in-situ at full load, and as a result, the remaining six NX6106XK-11 specimens which had not initiated - IN156, 57, 60, 61, 64, and 65 - were subjected to a brief (millisecond time frame) overload that produced ~0.05-0.5% plastic strain in most of these specimens as observed by DCPD. After the failed specimen was removed, testing was resumed at the original load, but because these specimens had been overloaded, the original load was no longer the current YS of the specimens. After a time span of 1772 hours at the original load, the load was slowly increased until the majority of the eight remaining specimens yielded. The remaining eight specimens began to initiate shortly thereafter. Additional SCCI tests could be conducted to make up for these likely non-representative initiation times for the NX6106XK-11 heat.

Heats 33375-2B, 522068, and WNP5 exhibited average SCCI times of 566, 653, and 417 hours, respectively, which are generally similar values. Three NX6106XK-11 specimens tested together exhibited a markedly lower average SCCI time of 240 hours. The distribution of initiation times, excluding the six suspect NX6106XK-11 times is shown in Figure 63. The four heats together exhibit a roughly normal distribution with a skewness of 0.94. The small amount of skewness that exists follows the same behavior as 15% CF Alloy 182 with the most probable SCCI time of approximately 450 hours being below the average SCCI time.

Initiation times for all four heats in the CF condition are significantly lower than for tests conducted on CR and CTS Alloy 600. SCCI times were 1,500-2,000 hours for tests at PNNL on 15-20% CR and 15-20% CTS NX6106XK-11 for the DOE-NE LWRS program [Zhai 2017]. This

suggests that the method of application of cold work may have a substantial effect on SCCI susceptibility just as was observed for Alloy 182.

Table 17. SCC initiation times of the 15% CF Alloy 600 materials. Mean, standard deviation, and median of all specimens is 518, 666, and 471 hours, respectively, after excluding the six suspect NX6106XK-11 initiation times.

33375-2B	S#	YS (MPa)	t_{init} (h)	NX6106XK-11	S#	YS (MPa)	t_{init} (h)
IN159	2	551	**1025**	IN156	1	544	**4600/2828***
IN162	3	547	**830**	IN157	1	547	**4591/2819***
IN163	3	558	**1062**	IN160	2	544	**3000/1228***
IN382	NA	551	**240**	IN161	2	547	**3205/1433***
IN383	NA	552	**403**	IN164	3	544	**3250/1478***
IN384	NA	554	**276**	IN165	3	547	**4100/2328***
IN385	NA	535	**495**	IN291	NA	516	**252**
IN386	NA	537	**350**	IN292	NA	515	**247**
IN387	NA	538	**413**	IN293	NA	521	**221**
Mean, S.D. Sample*			***566, 320***	***Mean, S.D. Sample***			***1426, 1060***
Median			***413***				***1433***
522068	**S#**	**YS (MPa)**	**t_{init} (h)**	**WNP5 CRDM**	**S#**	**YS (MPa)**	**t_{init} (h)**
IN224	NA	450	**880**	IN288	NA	497	**475**
IN225	NA	450	**890**	IN289	NA	494	**242**
IN226	NA	450	**840**	IN290	NA	501	**420**
IN304	NA	472	**508**	IN298	NA	509	**478**
IN305	NA	472	**550**	IN299	NA	514	**430**
IN306	NA	473	**725**	IN300	NA	509	**467**
IN307	NA	474	**477**	IN301	NA	509	**457**
IN308	NA	475	**525**	IN302	NA	512	**415**
IN309	NA	474	**483**	IN303	NA	511	**460**
Mean, S.D. Sample			***653, 179***	***Mean, S.D. Sample***			***427, 73***
Median			***550***	***Median***			***457***

S# String number if tested in a 3-string configuration.
† The ">" indicates not yet initiated. Test plan is to expose further if possible.
* These specimens spent 1,772 hours at ~90-96% of their YS. The lower number listed is the initiation time minus 1,772 hours and is the value used for statistical summaries.
** Statistical values based on exposure time of initiated and non-initiated specimens.

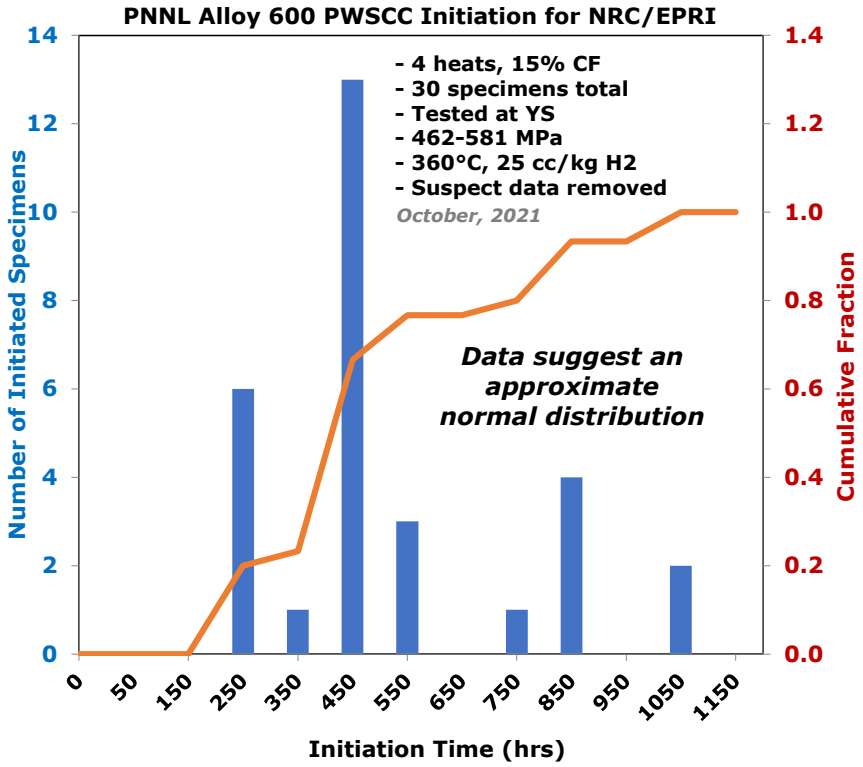

Figure 64. SCCI time distribution for four heats of 15% CF Alloy 600.

4.2 Alloy 600 Tests Conducted at Sub-Yield Stress Loading

The primary interest for these tests is to provide a comparison to Alloy 182 sub-YS SCCI behavior. As with Alloy 182, two heats – 33375-2B and WNP5 – were tested out of the four Alloy 600 heats used in this program. Tests were conducted at 90% and 80% of YS on either six or twelves specimens of each heat. The gauge surfaces were polished to a 1 µm finish to aid in identification of microstructural features on the surface of the specimens after SCC initiation. Testing was conducted in 360°C water at the Ni/NiO stability line (25 cc/kg H_2).

The actual test stress was not based on simply setting the target test stress to 90% of the YS values observed for the 100% YS test. This is because specimen-to-specimen variability in YS occurs, and there is always some variability in load cell accuracy. An additional metric that PNNL uses in setting the test stress for sub-YS tests is to target a particular plastic strain range. Analysis of SCCI tests conducted at 100% YS allowed the plastic strain range corresponding to 90% YS and 80% YS to be identified. When loading up specimens to sub-YS values, equal importance was applied to staying within the target plastic strain range and reaching the target test stress value.

For the 33375-2B specimens at 90% YS, a plastic strain range of 0.04-0.05% was expected to be reached at 90% YS, but a wider range of strain response occurred corresponding 0.04-0.13% plastic strain. The final stress range for 33375-2B 90% YS tests was 476-481 MPa which is estimated to be ~88% YS. For the 90% YS tests of the WNP5 specimens, the target plastic strain range was 0.06-0.07%. The attained plastic strain range was 0.04-0.09%. Final stresses were 440-447 MPa which are estimated to be ~89% YS. SCCI times of 15% CF Alloy 600 tested at 90% YS are summarized in Table 18.

For the 33375-2B specimens at 80% YS, a plastic strain of 0.02% was expected to be reached at 80% YS. The actual strains were 0.02-0.04%. The final stress range for 33375-2B 80% YS tests was 420-427 MPa which is estimated to be ~78% YS. For the 80% YS tests of the WNP5 specimens, the target plastic strain range was again 0.02%. The attained plastic strain range was 0.02-0.04% with final stresses of 400-407 MPa which are estimated to be ~81% YS. The 80% YS SCCI results are summarized in Table 19.

Table 18. SCC initiation times measured for 15% CF Alloy 600 tested at 90% YS. Only six tests are planned for 33375-2B. Mean, standard deviation, and median of all specimens is 673, 275, and 717 hours, respectively.

33375-2B (530-550 MPa YS)	**Test Stress (MPa)**	**Plastic Strain at Load (%)**	**t_{init} (h)**	**WNP5 CRDM (490-510 MPa YS)**	**Test Stress (MPa)**	**Plastic Strain at Load (%)**	**t_{init} (h)**
IN343	476	0.13	**910**	IN331	440	0.09	**150**
IN344	476	0.10	**1130**	IN332	440	0.05	**300**
IN345	477	0.05	**775**	IN333	440	0.06	**650**
IN346	479	0.03	**733**	IN334	441	0.06	**875**
IN347	479	0.06	**673**	IN335	441	0.08	**530**
IN348	481	0.06	**958**	IN336	442	0.06	**700**
				IN337	443	0.04	>913
				IN338	444	0.05	**525**
				IN339	445	0.06	**870**
				IN340	445	0.07	**850**
				IN341	447	0.07	**333**
				IN342	447	0.06	**240**
Mean, S.D. Sample		**863, 169**		***Mean, S.D. Sample***		**578, 273**	
Median		**843**		***Median***		**590**	

† The ">" indicates not yet initiated. Test plan is to expose further if possible.
** Statistical values based on exposure time of initiated and non-initiated specimens.

Table 19. SCC initiation times measured for 15% CF Alloy 600 tested at 80% YS. Mean, standard deviation, and median of all specimens is 1,225, 487, and 1,244 hours, respectively.

33375-2B (530-550 MPa YS)	**Test Stress (MPa)**	**Plastic Strain at Loading (%)**	**t_{init} (h)**	**WNP5 CRDM (490-510 MPa YS)**	**Test Stress (MPa)**	**Plastic Strain at Loading (%)**	**t_{init} (h)**
IN349	420	0.025	**590**	IN400	400	0.035	**535**
IN350	422	0.025	**1454**	IN401	402	0.02	**722**
IN351	421	0.03	**1410**	IN402	402	0.04	**890**
IN352	422	0.02	**2143**	IN403	404	0.02	**1252**
IN353	427	0.04	**1236**	IN404	405	0.025	**1635**
IN354	426	0.03	**1107**	IN405	407	0.02	**1731**
Mean, S.D. Sample		**1323, 508**		***Mean, S.D. Sample***		***1128, 492***	
Median		**1323**		***Median***		***1071***	

A plot of SCCI time versus applied stress below the YS is provided in Figure 64. Unlike 15% CF Alloy 182, 15% CF Alloy 600 readily undergoes SCCI even at 80% YS loading. This is yet another indicator the Alloy 600 exhibits fundamentally different SCCI behavior than Alloy 182. A power law curve fit to the data produces an average stress exponent of 3.4 for the two heats.

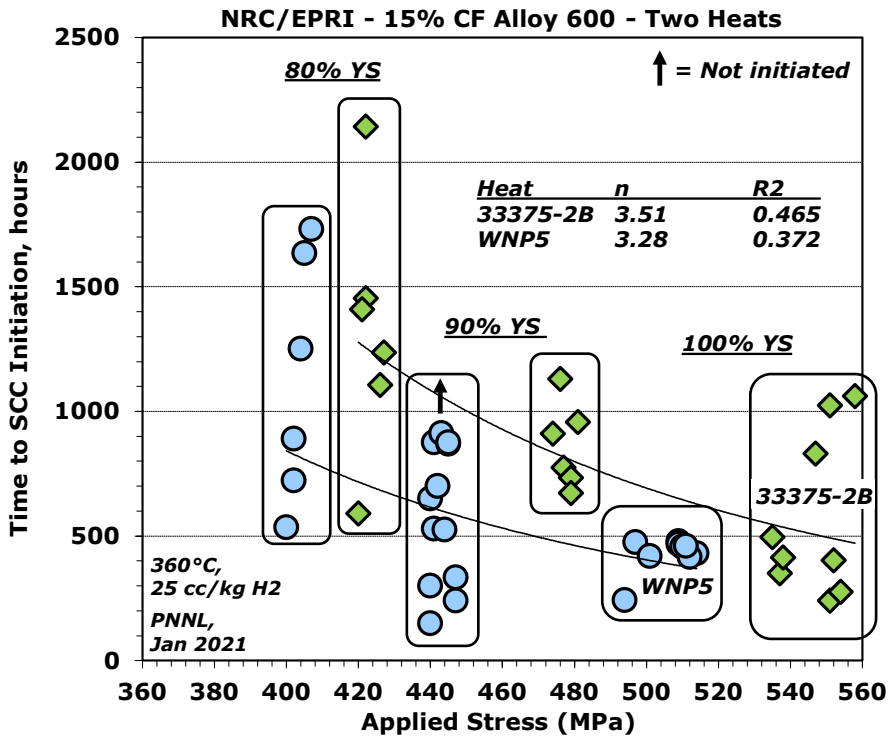

Figure 65. SCCI time versus applied stress of 15% CF Alloy 600.

5.0 Summary of Testing Observations

5.1 Alloy 182

Trends observed from the Alloy 182 SCCI test results are as follows:

- The as-welded Alloy 182 specimens made from four different weld mockups did not exhibit DCPD-detected initiation after 5.1 years of exposure at 360°C. However, post-test specimen examinations revealed what appear to be shallow surface cracks in several specimens that did not result in detectable initiations. In contrast, non-CW Alloy 600 readily exhibits SCCI at the same test temperature. Non-CW Alloy 600 SCCI tested at PNNL for the DOE-NE LWRS program often exhibited SCCI in less than one year, while data in the literature indicate values of approximately two years. There are several significant differences in composition and microstructure between Alloy 182 and Alloy 600, but none of the differences readily explain this difference in SCCI behavior.
- PWSCC initiation of Alloy 182 is highly dependent on the mode of deformation applied to the material. While 15% CF Alloy 182 exhibits sub-100 hour SCCI times, 15% CTS Alloy 182 did not exhibit SCCI after two years of constant load exposure. Because of this difference, the stress exponent for SCCI of Alloy 182 varies strongly with the mode of deformation applied to the material. SCCI of CF Alloy 182 has a very strong stress dependence, which results in a large stress exponent of approximately 12. The much weaker stress dependence of CTS Alloy 182 results in a much lower stress exponent. The stress exponent of CTS Alloy 182 based on literature data is 4.3, while the stress exponent estimated from the PNNL cold tensile strain Alloy 182 data is lower than 4.3.
- As covered in the previous Alloy 182 report, 15% CF Alloy 182 tested at 90% YS exhibits much longer SCCI times than when tested at its YS. Eleven out of twelve specimens tested at 90% YS exhibited SCCI times greater than 10,000 hours, whereas the same materials tested at their YS had initiation times below 100 hours.
- 15% CF Alloy 182 SCCI exhibits a much different temperature dependence than 15% CF Alloy 600. As test temperature is reduced from 360°C to 300°C, the long tail in the distribution of SCCI times of Alloy 182 vanishes, causing the distribution of initiation times at lower temperatures to become more uniform. For the Studsvik Alloy 182, the shortest SCCI times increased as the test temperature decreased, however for the Phase 2B Alloy 182, the shortest SCCI times at 330°C are the same as at 360°C. The changing shape of the SCCI time distribution curve as a function of test temperature makes it a challenge to determine an activation energy. Using the average initiation time gives a negative activation energy. However, using the median or most probable SCCI time gives a positive activation energy, which is typical for the temperature dependence of SCC for many alloys.
- Scoping tests to evaluate the DH dependence on 15% CF Alloy 182 SCCI have revealed a similar trend observed for Alloy 600 SCCI in the literature, namely that there may be a tendency for longer SCCI times in the NiO-stable regime and lower SCCI times in the Ni-metal stable regime.

5.2 Alloy 600

Trends observed in the Alloy 600 SCCI behavior based on the current test results are as follows:

- Among the four heats of Alloy 600 tests in a 15% CF condition, 360°C initiation times at the YS are relatively consistent when excluding the six long initiation times for NX6106XK-11. The average of all four heats is 518 hours, while the median is 666 hours. The skewness of heats 33375-2B and 522068 are 0.78 and 0.43, which represent a fairly uniform distribution of SCCI times, while for WNP5, the skewness is -2.44 which was caused by one specimen with a short initiation time. The most probable initiation time is only slightly lower than the average.
- The effect of the mode of applied deformation on SCCI times for Alloy 600 appears to be the same as for Alloy 182, namely that cold forging in compression and then testing in tension along the same deformation direction results in much shorter SCCI times than when deforming and testing in tension.
- 15% CF Alloy 600 readily undergoes SCCI at sub-YS loadings. The stress exponent in this sub-YS loading range was observed to be approximately 3.4.
- The sub-YS loading SCCI behavior of 15% CF Alloy 600 is clearly different from the 15% CF Alloy 182. For example, testing 15% CF Alloy 182 at 90% of the yield strength increased the SCCI time by 6.6x based on average initiation time and 13x based on median initiation time. However, 15% CF Alloy 600 tested at 80% and 90% of the yield strength resulted in less than a 2x increases in SCCI time at both test stresses.

6.0 References

Azatyan, V.V., Petukhov, V.A., Prokopenko, V.M. , Timerbulatov, T.R. (2019), "Possible Gravitational Stratification of Components in Mixtures of Reaction Gases", Russian Journal of Physical Chemistry A **93**(5): 777-778.

Berge, J.P. (1997), "Importance of surface preparation for corrosion control in nuclear power stations", Materials Performance **36**(11): 56-62.

Bickel, D.R. (2002), "Robust estimators of the mode and skewness of continuous data", Computational Statistics & Data Analysis **39**(2): 153-163. 10.1016/s0167-9473(01)00057-3

Bickel, D.R. , Frühwirth, R. (2006), "On a fast, robust estimator of the mode: Comparisons to other robust estimators with applications", Computational Statistics & Data Analysis **50**(12): 3500-3530. 10.1016/j.csda.2005.07.011

Bruemmer, S.M., Olszta, M.J., Schreiber, D.K. , Toloczko, M.B. (2014), “Stress Corrosion Crack Initiation of Cold-Worked Alloy 600 and Alloy 690 in PWR Primary Water”, U.S. Department of Energy - Nuclear Energy, M2LW-14OR0404023.

Dinh, L.N. , McLean II, W. (2020), “Mixed gases in compressed cylinders: some popular misconceptions and explanations”, Lawrence Livermore National Laboratory, LLNL-TR-812248.

Etien, R.A., Richey, E., Morton, D.S. , Eager, J. (2011), "SCC initiation testing of alloy 600 in high temperature water", 15th International Conference on Environmental Degradation of Materials in Nuclear Power Systems - Water Reactors, Colorado Springs, CO, USA, The Minerals, Metals & Materials Society.

Furstenau, R. (2021), Memorandum OF Understanding between U.S. Nuclear Regulatory Ccmmission and Electric Power Research Institute, Inc. on Cooperative Nuclear Safety Research.

Grenander, U. (1965), "Some Direct Estimates of the Mode", The Annals of Mathematical Statistics **36**(1): 131-138. 10.1214/aoms/1177700277

Le Hong, S., Amzallag, C. , Gelpi, A. (1999), Modelling of stress corrosion cracking initiation of Alloy 600 in primary water of PWRs, 9th International Symposium on Environmental Degradation of Materials in Nuclear Power Systems - Water Reactors, Newport Beach, California, The Minerals, Metals & Materials Society**:** 115-123.

Morton, D.S., Attanasio, S.A. , Young, G.A. (2001), “Primary Water SCC Understanding and Characterization Through Fundamental Testing in the Vicinity of the Nickel/Nickel Oxide Phase Transition”, LM-01KO38.

Scott, P., Meunier, M.C., Steltzlen, F., Calonne, O., Foucault, M., Combrade, P. , Amzallag, C. (2007), "Comparison of laboratory and field experience of PWSCC in alloy 182 weld metal", 13th International Conference on Environmental Degradation of Materials in Nuclear Power Systems - Water Reactors, Whistler, BC, Canada, Canadian Nuclear Society, The Minerals, Metals & Materials Society.

Toloczko, M.B., Deibler, J., Smart, J.E. , Bouffioux, R.A. (2020), “PNNL 4-Point Bend SCC Test Method Development for the U.S. Nuclear Regulatory Commission”, Pacific Northwest National Laboratory, PNNL-29710.

Toloczko, M.B., Olszta, M.J., Zhai, Z. , Bruemmer, S.M. (2015), "Stress corrosion crack initiation measurements of alloy 600 in PWR primary water", 17th International Conference on Environmental Degradation of Materials in Nuclear Power Systems - Water Reactors, Ottawa, ON, Canada, Canadian Nuclear Society.

Toloczko, M.B. , Zhai, Z. (2017), “Materials Reliability Program: Stress Corrosion Crack (SCC) Initiation Testing of Ni-Base Alloys for PWR Applications - Part 1 (MRP-426)”, Electric Power Research Institute, Product #3002010761.

Toloczko, M.B., Zhai, Z., Wang, J., Olszta, M.J. , Bouffioux, R.A. (2021a), “Materials Reliability Program: Stress Corrosion Crack (SCC) Initiation Testing of Ni-Base Alloys for PWR Applications Part 2 (MRP-448)”, Electric Power Research Institute, Electric Power Research Institute, EPRI Report #3002018002.

Toloczko, M.B., Zhai, Z., Wang, J., Olszta, M.J. , Bouffioux, R.A. (2021b), “PWSCC Initiation Testing of Ni-base Alloys, Report 2”, Pacific Northwest National Laboratory, PNNL-31016.

Troyer, G., Fyfitch, S., Schmitt, K., White, G. , Harrington, C. (2015), "Dissimilar metal weld PWSCC initiation model refinement for xLPR part I: a survey of alloy 82/182/132 crack initiation literature", 17th International Conference on Environmental Degradation of Materials in Nuclear Power Systems—Water Reactors, Ottawa, ON, Canada.

White, G. (2002), “Materials Reliability Program (MRP) Crack Growth Rates for Evaluating Primary Water Stress Corrosion Cracking (PWSCC) of Thick-Wall Alloy 600 Materials (MRP-55) Revision 1”, Electric Power Research Institute, Palo Alto, CA, 1006695.

White, G. (2004), “Materials Reliability Program Crack Growth Rates for Evaluating Primary Water Stress Corrosion Cracking (PWSCC) of Alloy 82, 182, and 132 Welds (MRP-115)”, Electric Power Research Institute, Palo Alto, CA, 1006696.

Zhai, Z. , Toloczko, M.B. (2023), “FY 2023 Progress on Stress Corrosion Crack Testing of Ni-Base Alloys in PWR Primary Water”, U.S. Department of Energy - Nuclear Energy, M2LW-23OR04020311.

Zhai, Z., Toloczko, M.B., Olszta, M.J. , Bruemmer, S.M. (2017), "Stress corrosion crack initiation of alloy 600 in PWR primary water", Corrosion Science **123**: 76-87. https://doi.org/10.1016/j.corsci.2017.04.013

Zhai, Z., Wang, J., Toloczko, M.B. , Bruemmer, S.M. (2020), “Evaluation of Critical Parameters to Model Stress Corrosion Crack Initiation in Alloy 600 and Alloy 182 in PWR Primary Water”, U.S. Department of Energy - Nuclear Energy, M2LW-20OR0402036.

Pacific Northwest National Laboratory

902 Battelle Boulevard
P.O. Box 999
Richland, WA 99354
1-888-375-PNNL (7665)

www.pnnl.gov